Nationaal Onderzoeksprogramma
Broeikasgassen
Veenweiden

Chapter 11 NOBV year report 2022

Process-based modelling of CO_2 fluxes in Vlist

Process-based modelling of CO_2 fluxes in Vlist

Authors

D. van de Craats[1], M. van den Berg[2], Jacobus van Huissteden [2], Ype van der Velde [2], Jim Boonman[2]

Affilitation

[1]Wageningen Environmental Research, WAGENINGEN

[2]Vrije Universiteit, AMSTERDAM

Reviewers: Roel Melman (Deltares)

Abstract

To distinguish processes affecting CO_2 emissions and to disentangle sources contributing to these emissions, the process-based models PEATLAND-VU and SWAP-ANIMO were applied to the NOBV location Vlist. CO_2 fluxes and other environmental variables were modelled for both the reference and PWIS parcel, of which the latter was equipped with a passive water infiltration system (PWIS; submerged drains) to allow for extra water infiltration in summer. Model outcomes were compared to measurements of chamber CO_2 fluxes (with a high temporal resolution) and long-term soil subsidence measurements, and to results of the PP2D-AAP and HYDRUS-AAP models for the same location.

Model results generally show good agreement with measured hydrological variables and CO_2 fluxes throughout the year. The net ecosystem carbon balances (NECB), determined with the two models are in good agreement with the measured chamber NECB for the year 2020. For the year 2021 the modelled NECB is slightly higher for the reference parcel (~2 t CO_2 ha^{-1} yr^{-1}) and PWIS parcel (~3-4 t CO_2 ha^{-1} yr^{-1}) than the measured NECB. This leads to differences in measured and modelled CO_2 emission reductions in the parcel with PWIS compared to the reference. An emission reduction of 6.6 (31%) and 3.1 (25%) t CO_2 ha^{-1} yr^{-1} was found with chamber measurements for 2020 (dry) and 2021 (wet), respectively, compared to 4.8 (24%) and 0.7 (5%) t CO_2 ha^{-1} yr^{-1} for PEATLAND-VU, and 3.9 (21%) and 0.9 (7%) t CO_2 ha^{-1} yr^{-1} for SWAP-ANIMO for the same years. Reductions from PP2D-AAP (0.6 and –0.5 t CO_2 ha^{-1} yr^{-1} (3 and -3 %)) and HYDRUS-AAP (6.2 and –0.5 t CO_2 ha^{-1} yr^{-1} (28 and -4 %)) form the outer model prediction bounds in 2020 and predict an increase in emission from the PWIS parcel in 2021.

Accounting for CO_2 emission derived from peat oxidation only, the modelled emission is lower than the modelled NECB: 14.1 and 12.9 t CO_2 ha^{-1} yr^{-1} (compared to an NECB of 17.0 and 14.3 t CO_2 ha^{-1} yr^{-1}) for the reference and PWIS parcel for PEATLAND-VU, respectively, and 14.9 and 13.4 t CO_2 ha^{-1} yr^{-1} (compared to an NECB of 17.9 and 15.5 t CO_2 ha^{-1} yr^{-1}) for the reference and PWIS parcel for SWAP-ANIMO, averaged over the two years. This is very well comparable with ten years of soil subsidence measurements in Vlist converted to CO_2, with an average emission of 12 t CO_2 ha^{-1} yr^{-1}. The emission reduction from the PWIS parcel for peat oxidation is 2.4 and 0.0 t CO_2 ha^{-1} yr^{-1} for PEATLAND-VU, and 2.8 and 0.3 t CO_2 ha^{-1} yr^{-1} for SWAP-ANIMO for 2020 and 2021. This is also comparable to the estimated reduction of 1.1 t CO_2 ha^{-1} yr^{-1} based on the long-term soil subsidence.

Highlights

- The process-based models PEATLAND-VU and SWAP-ANIMO have successfully been used to model CO_2 fluxes in Vlist.
- Modelled reductions in net ecosystem carbon balance from the field with submerged drains relative to the reference field are lower as compared to measured reductions.
- Modelled peat decomposition is in range with long-term soil subsidence measurements.

Process-based modelling of CO_2 fluxes in Vlist

1 Introduction

Measuring carbon dioxide (CO_2) exchange between ecosystem and atmosphere is a widely used method to determine peat oxidation from drained peat soils. The net ecosystem carbon balance (NECB), which is the net ecosystem exchange (NEE), or net CO_2 flux, over a year with accounting for yield and manure application (Figure 1), is generally taken as an estimate for peat oxidation. This might be the case if the short-term carbon cycle, dominated by vegetation, is in balance within one year. The carbon processes are, however, often complex and determined by weather conditions and interactions between different carbon pools, and it is likely that also short-term carbon cycles are not exactly in balance over one year. Process-based models may be used to better estimate the contribution of the soil carbon pools, including peat oxidation, to the measured CO_2 fluxes both within a season or a year and over multiple years.

There is a wide range of models that simulate carbon transfers from soil to atmosphere. These vary in scale, from plot scale to soil submodels in Earth System models, and in complexity with respect to the processes included (Van Huissteden, 2020). Also, the scope of the models may differ, with a focus on agricultural land use or natural ecosystems. For the purpose of the NOBV project, models that include the peat carbon reservoir (being also a part of the soil matrix) are relevant, with a plot or parcel spatial scale, and a capability to include at least agricultural processes such as harvest or grazing. There are several models that could fulfil these requirements, eventually with adaptations, e.g., ECOSSE (Smith et al., 2010) and COUP (Jansson and Karlberg, 2004; Metzger et al., 2015). Metzger et al. (2015) give a more extensive list of similar soil carbon models.

Within this study we used two similar process-based models, PEATLAND-VU (van Huissteden et al., 2006, 2009) and SWAP-ANIMO (Kroes et al., 2017, Groenendijk et al., 2005) to model the (hydrology and) carbon dynamics for the NOBV field site Vlist. The advantage of these models is that they have been tested before in Dutch peatland settings and for a wider range of soil carbon applications (e.g., for Peatland-VU: Van Huissteden et al., 2006; Petrescu et al., 2010; Metzger et al., 2015; for SWAP-ANIMO: Hendriks et al., 2008; Stolk et al., 2011; Hendriks & van den Akker, 2012; Hendriks et al., 2013). Moreover, the models have been developed by NOBV project partners, which facilitates adaptation of the models if needed. Also, these two models form part of the ensemble modelling system SOMERS (Erkens et al., 2022). Therefore, they are also compared with the (conceptually simpler) PeatParcel2D-AAP (PP2D-AAP), as part of SOMERS, and HYDRUS-AAP (Boonman et al., 2022) models. The latter two models only simulate peat oxidation based on modelled temperature and soil moisture, and convert this to a CO_2 emission based on empirical relations (HYDRUS-AAP) or soil carbon content and measured soil respiration rates (PP2D-AAP). With this, other soil organic matter pools, such as vegetation, are ignored. The advantage of these models is that run time and data requirements allow for an easier usage of these models on a larger (national) scale. It is, however, not possible to directly compare the model results of these two models to measured CO_2 data, except for the comparison with NECB. But as described above, several measurement years are needed to be able to use NECB as measure for peat oxidation.

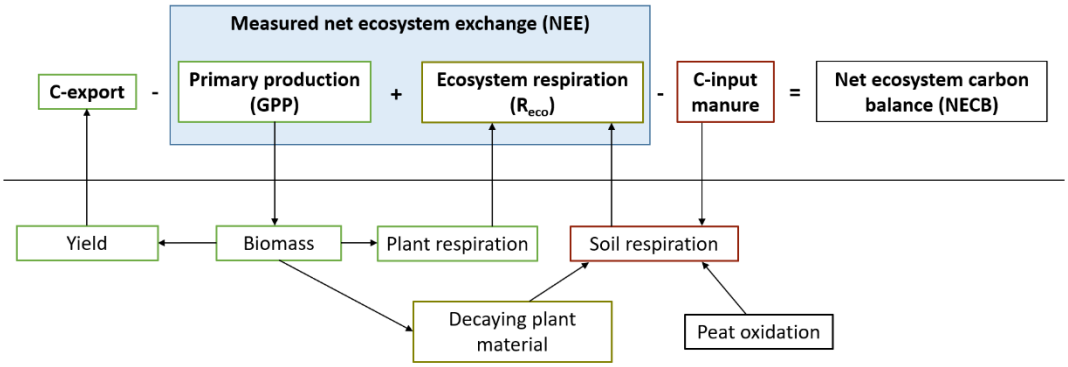

Figure 1 Simplified schematic overview of the components that contribute to the different measured and partitioned carbon fluxes (C-export, GPP and R_{eco}), which sums up to the NECB. Soil respiration consists of both young, plant and manure derived carbon, and old (fossil), peat derived carbon.

Both the process-based models, PEATLAND-VU and SWAP-ANIMO, have a 1D spatial dimension and contain submodels for soil physics (water table, soil temperature and soil moisture), biomass production and CO_2 production. CO_2 production is the sum of plant respiration and decomposition from different soil organic matter (SOM) pools, like litter, root exudates, dissolved organic matter, microbial biomass, humus and peat. There are differences between the models, mainly within the soil physical and biomass production submodels (see sections 3.1 and 3.2). Smaller differences exist in the SOM pools and decomposition calculations. Decomposition in SWAP-ANIMO is for instance related to oxygen availability, which is directly modelled with oxygen transport, while with PEATLAND-VU this relation is more indirectly modelled as function of water filled pore space (WFPS). The models are developed for drained (not permanently saturated or flooded) conditions. We calibrated the models for NOBV field site Vlist, an intensively used drained peat meadow site, for the years 2020 and 2021. For the SWAP-ANIMO model, only a view parameters were optimized, most parameters were gained from literature, lab or field measurements. For PEATLAND-VU the aim was to create an optimal parameter set for drained peat meadows, so a more extensive calibration procedure was done (see 2.1 and 2.2). On this site there are two parcels with different water management regimes and each parcel is equipped with automatic flux chambers and sensors for relevant environmental variables.

The aim of this study is to evaluate the performance of the two models in simulating the measured CO_2 flux on a daily and annual basis. For this, also model performance on state variables assumed to drive the CO_2 flux are evaluated. The measured CO_2 fluxes are partitioned into ecosystem respiration (R_{eco}) and gross primary production (GPP) (Figure 1), and model results are compared to that. An estimate for peat oxidation and how the different water table regimes affect it, is made with both models. The model performances on a yearly base are put into perspective of other modelling estimates used within the NOBV (PP2D-AAP, HYDRUS-AAP) and with long-term soil subsidence measurements.

2 Abbreviations

AAP	Aerobic assimilation potential
BR	Basal respiration
DOC	Dissolved organic carbon
DOM	Dissolved organic matter
FOM	Fresh organic matter
GPP	Gross primary production
LHM	Landelijk Hydrologisch Model
LOI	Loss on ignition
MS	Measure parcel (parcel with PWIS)
NECB	Net ecosystem carbon balance
NEE	Net ecosystem exchange
OM	Organic matter
PSO	Particle swarm optimalisation
PWIS	Passive water infiltration system
R_{eco}	Ecosystem respiration
R_{plant}	Plant derived respiration
R_{soil}	Soil derived respiration
RF	Reference parcel
RMSE	Root mean squared error
SOM	Soil organic matter
WFPS	Water filled pore space

3 Model descriptions

3.1 PEATLAND-VU (PL)

The PEATLAND-VU model represents a 1.5 m deep 1D soil column with a specified surface level and consists of 15 layers with a constant thickness of 0.1 m. For each layer, the following is described: pH, organic matter content, C/N ratio, dry bulk density, sand fraction of mineral fraction, water retention curve parameters and freezing curve (optional). An overview of the organic matter pools and fluxes considered in the model is given in Figure 2.

Soil physical conditions are the basis for the plant production and SOM decomposition modules. Soil temperature is calculated by varying thermal diffusivity within each soil layer, dependent on soil moisture, volumetric heat capacity and thermal conductivity. Soil moisture is assumed to be in equilibrium with gravity. Changes in soil moisture due to evapotranspiration and precipitation cannot be simulated. Groundwater levels can be modelled, but in this study measured data are used as input for the model. It is also possible to import WFPS data in PEATLAND-VU from other models (or measurements), but this was not done in this study.

PEATLAND-VU contains three different plant production models. The one used for this study is described in Shaver et al. (2007), with some slight adaptations. It models gross primary production (GPP) and plant respiration (R_{plant}). GPP minus plant respiration is the net primary production.

The leaf area index (LAI) is separately calculated and is used in the model to calculate GPP and R_{plant}. For LAI plant phenology is used: growing degree days, maximum LAI, start and end of growing season and fraction of leavy biomass that is littered in autumn. The development of the plant (= increase in LAI) in the beginning of the season is depending on the growing degree days (temperature based) and after that on the primary production (light intensity based).

The addition of fresh organic material (FOM) to the root zone is modelled with an above and below ground primary production relation dependent on soil temperature in the upper 10 cm. If the top layer is close to saturation, an oxygen reduction factor is applied which reduces GPP. Primary production is partitioned in above and belowground biomass, and part of the belowground biomass goes to the loss of carbon in the form of root exudates. Exudate release is higher for younger roots (Whipps, 1990) and is therefore higher in spring, represented in the model with a spring correction. Above and below ground biomass dies off every time step, that allocates the carbon to the roots/litter SOM pool. During harvest, a fraction of the aboveground biomass is removed from the system.

The decomposition of SOM pools is assumed to be partitioned between CO_2, microbial biomass and humus pool following first order kinetic and a decomposition rate constant. The amount of organic carbon that is partitioned to the microbial biomass is determined by the microbial assimilation rate, the same accounts for the humus pool and the rest is transferred into CO_2. The microbial biomass is decomposed as well, depending on the death rate and decomposition of its dead organic material. Decomposition rate of each pool is depending on environmental factors as soil moisture, temperature, pH, priming effect, and in case of peat decomposition also on the C/N ratio.

The model was calibrated with the particle swarm optimalisation (PSO) method (Clerc, 2011), making use of the R-package hydroPSO ('spo2011'). Optimization was forced towards the lowest standardized root mean square error (RMSE). A swarm size of 70 was chosen and a maximum number of iterations of 1000. The calibration was done for the measuring years 2020-2021, with a spin up period of 10 years to ensure stable soil carbon pools. The model was calibrated on R_{eco}, GPP, yield and cumulative NEE simultaneously, with the highest weight for R_{eco} and GPP (0.3) followed by yield (0.25) and cumulative NEE (0.15).

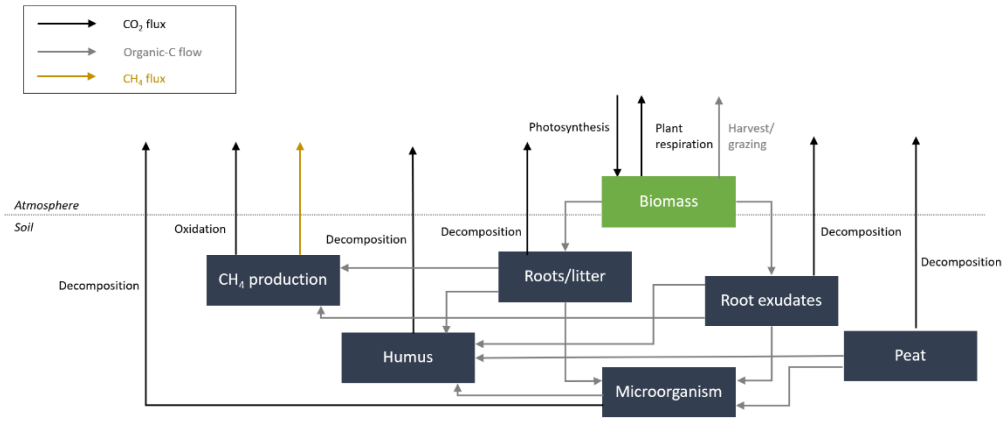

Figure 2 Schematic overview of the PEATLAND-VU model with soil organic matter (SOM) pools, CO_2 and CH_4 fluxes, and organic carbon flows from one pool to the other.

3.2 SWAP-ANIMO (SA)

The SWAP model (Kroes et al., 2017) is used to model processes as vertical soil water flow (Richard's equation) and heat transport, drainage and infiltration, evapotranspiration and crop growth in a pseudo-2D approach. The model considers a one-dimensional soil column with increasingly coarse cell sizes with depth. A number of soil horizons are distinguished based on field and laboratory measurements, for which Mualem-Van Genuchten parameters (Mualem, 1976; Van Genuchten, 1980) are defined. Field scale lateral drainage and infiltration to and from the ditch and tile drains, and drainage from the field trench are modelled based on calibrated drainage and infiltration resistances. The resulting hydrological output is field averaged.

Grass growth is simulated with the detailed grass module in SWAP, which is based on the WOFOST model (Boogaard et al., 2014). It provides estimates of gross primary production (GPP), plant respiration (R_{plant}) and grass yield. GPP is a function of yearly averaged atmospheric CO_2 concentrations and daily data on radiation, temperature, crop characteristics and actual crop development. The potential GPP may be reduced to a maximum attainable GPP by multiplication with a (calibrated) stress factor to account for nutrient limitations or pests. The attainable GPP may be further reduced to an actual GPP due to soil moisture conditions as drought or oxygen stress in the root zone. Kroes & Supit (2011) suggest a stress factor of 0.8 for the nutrient application rates at the field sites.

It is assumed that carbon taken up during the day is first allocated to maintenance respiration, as function of biomass and temperature. Any remaining carbon is then partitioned between the individual grass components (roots, leaves and stems). Part of the carbon is lost as growth respiration during this process, as determined by the assimilation efficiency. Roots, leaves and stems each have their own partitioning, assimilation and maintenance respiration factors. In addition to the process of growth, part of the living biomass may die due to senescence or water stress, and harvest of above ground biomass occurs at prescribed dates. Root exudates are not considered explicitly but are implicitly incorporated in root assimilation efficiency and maintenance respiration factors. Root exudates, therefore, do not influence the soil organic matter cycles.

Daily SWAP output is used as input for the ANIMO model (Groenendijk et al., 2005) to simulate belowground C (carbon) and N (nitrogen) processes. We only present the carbon cycle in this report. Carbon is present in organic matter (OM) with a fixed fraction for all types of OM. The model considers a variety of OM pools (Figure 3). Each pool has user defined potential dissimilation rates, partitioning factors, assimilation efficiencies and nitrogen contents. These parameters were partly standard, and partly calibrated for the current model application.

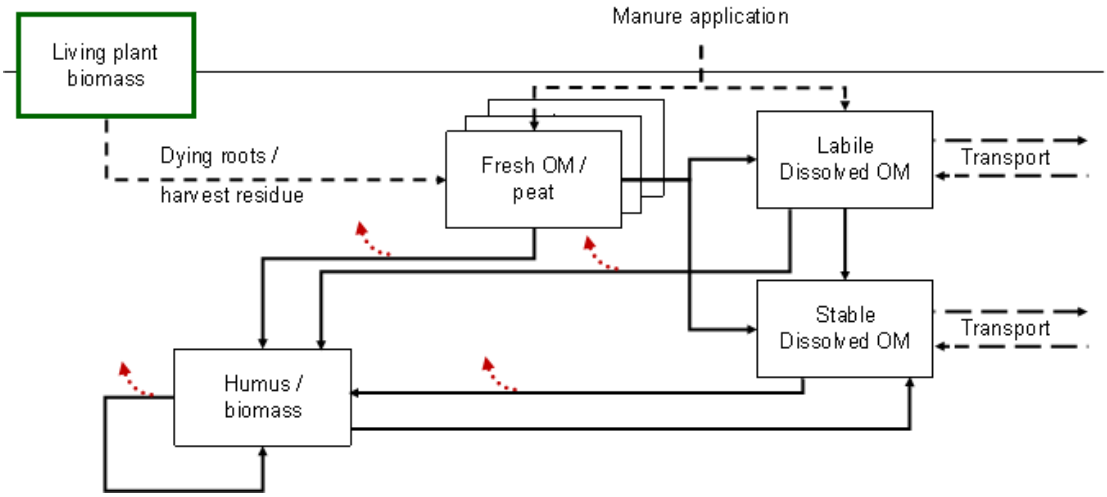

Figure 3 Organic matter pools and transport (dashed) - and decomposition (solid) pathways in the ANIMO model. Red dotted lines indicate CO_2 respiration pathways.

Multiple fresh organic matter (FOM) pools are distinguished, which each have their own properties regarding e.g. decomposition rate or nitrogen content. They may be replenished by dying roots, harvest residues or manure. In the current application, two FOM pools are reserved for peat, one fast decomposing, and one slowly decomposing pool, which are both not replenished. FOM can be decomposed to dissolved organic matter (stable or labile DOM pool), or in humus/microbial biomass. DOM can be transported both vertically and horizontally as dictated by SWAP output and can be decomposed to the humus/biomass pool. This pool consists of both living microbial biomass and humus. Root exudates and priming effects are not considered in ANIMO for grassland. CO_2 is formed during dissimilation of FOM to humus, DOM to humus as well as during the turnover of the humus pool. It is assumed to escape to the atmosphere directly. An overview of all transport – and decomposition pathways of carbon considered in the model are given in Figure 3.

Decomposition of OM from each pool and depth depends on (pool specific) potential dissimilation rates, substrate availability and response factors. The definitions of potential dissimilation rates and substrate availability were based on a combination of measurements, calibration and initialisation runs. The response factors include effects of acidity (static in time), temperature, drought and oxygen limitation, which all vary with depth. Oxygen transport is modelled explicitly by considering both transport and consumption of oxygen required for decomposition. In case oxygen is not available for decomposition, nitrate (modelled explicitly as well) may be used as alternative electron acceptor to fulfil the oxygen demand for decomposition processes. If both are absent, no decomposition is simulated as alternative acceptors are not considered in the current model version of ANIMO. This approach deviates from the other models in this report, where water filled pore space (WFPS) is used to describe both drought and oxygen limitation stress and where only aerobic decomposition is considered.

The model pools are initialized with historical simulations of the site from 1960 onwards. Initial conditions are prescribed based on (current) peat densities (see 11.3.2), and it is assumed that a fraction of 2/3 of the OM is slowly decomposable peat, and 1/3 is fast decomposable, similar as in Hendriks et al. (2008). As decomposing peat results in a lowering of the field surface, it is assumed that ditch water levels are lowered in accordance with the loss of organic matter every ten years. In modelling terms, OM is moved up in the soil profile once every ten years to account for the losses of OM over time. An extended overview and discussion of all parameter input values used in this study and deviating from standard values can be found in the Appendix (section 10.2).

3.3 HYDRUS-AAP (HA)

The effect of different water management strategies on net carbon emissions was analysed for two NOBV locations (Assendelft and Vlist) in the study of Boonman et al. (2022), assuming that only soil moisture (WFPS) and soil temperature drive net CO_2 emissions. Hydrological conditions and temperature in both the saturated and unsaturated zone were modelled in space and time with the 2D HYDRUS model (Šimunek et al., 2022). The aerobic assimilation potential (AAP) was defined to translate model results to CO_2 emission. The AAP is equal to 1 for optimal conditions (soil temperature of 20°C and WFPS of 0.65) and decreases with decreasing temperature and with water filled pore space (WFPS) moving away from this optimum in either direction. Integration of the AAP over each model node and dividing by domain length gives the field average potential CO_2 respiration rate per area (in d m). Integrating this over a year gives the total yearly field averaged aerobic assimilation potential (AAP_{yr}). As detailed in Boonman et al. (2022), an empirical relation with measured NECB in Assendelft and Vlist (derived from automated chamber measurements) was established (Eq. 1) as

$$NECB = 2.6 + 0.32AAP_{yr}, \quad (1)$$

with NECB in t CO_2 ha^{-1} yr^{-1} and AAP_{yr} in d m yr^{-1}. Overall, the authors found a strong relation between NECB and AAP_{yr}. For a more detailed description, see Boonman et al. (2022). Here, we use Eq. (1) to obtain a yearly estimate of the NECB based on the modelled AAP_{yr}

3.4 PP2D-AAP (PA)

Another method was developed to model the influence of e.g. parcel width, ditch levels and the application of drains on peat oxidation, described in Erkens et al. (2022). The hydrological model (PeatParcel2D; PP2D) consists of a (saturated zone) 2D MODFLOW model (Langevin et al., 2017) which, in the version used for this study, is parameterized as described in Erkens et al. (2022). The groundwater level at one-third of the parcel width is taken as field average water level. To obtain WFPS at this position, a fixed relation between groundwater level and WFPS as function of depth is assumed based on simulations with HYDRUS presented in Boonman et al. (2022). A summer and winter temperature as function of depth are prescribed based on averages of soil temperature measurements in NOBV locations Assendelft, Aldeboarn, Rouveen and Zegveld. A similar description of the AAP is used in PP2D-AAP as in HYDRUS-AAP. The yearly total AAP is now calculated based on an integration over only depth and time. However, the translation to peat oxidation differs between both approaches. The daily carbon emission per model cell in PP2D-AAP is given as

$$CO_2e = AAP * m_{om} * BR, \quad (2)$$

where CO_2e [µg CO_2 d^{-1}] is the CO_2 emission rate at each model cell, AAP [-] is the aerobic assimilation potential, m_{om} [g OM] is the organic matter mass and BR is the basal respiration, which was set at 313.83 µg CO_2 gOM^{-1} d^{-1} based on the mean of measurements of respiration rates of soil samples from Aldeboarn, Vlist, Rouveen and Zegveld within NOBV. The organic matter mass is derived from the soil map of the Netherlands by using empirical relations between relative organic matter content and organic matter density. Integrating Eq. 2 over the model depth and over time yields an estimate of the yearly NECB. The methodology is further detailed in Erkens et al. (2022).

4 Methods

4.1 Site description

The research location considered is situated in Vlist (51.98 N, 4.82 E), in the province Zuid-Holland, the Netherlands. This area is characterized by extensive peat meadow areas, which are partly covered by clay deposits from nearby rivers. Most of the area is in use as intensively managed perennial grassland for dairy farming. To allow for optimal soil water conditions for productive farming, a dense network of ditches with relatively fixed water levels was created centuries ago. Parcels are long (few hundred meters) but narrow (20 to 50 m wide) to facilitate fast drainage (winter) and some infiltration (summer) of water. As a result of drainage, the soil is subsiding due to oxidation of organic matter, but also (irreversible) shrinkage and consolidation play a role. Over the course of time, the parcels have become slightly hollow due to differential subsidence and dredging of ditches, adding material to the side of the parcels.

The research location is a typical field for this area, with a parcel width of 35 m and a trench of 20-30 cm deep in the middle to facilitate drainage from the middle of the slightly hollow field. The water levels of the adjacent ditches are managed to summer and winter levels of 50 and 60 cm below average field surface, respectively. A clay layer of 35-45 cm thick is situated on top of a somewhat degraded layer (40-60 cm), followed by thick, more pristine layers of peat, alternated with clay layers deposited in times of flooding. Around five times a year grass (*Lolium perenne*) is mowed for dairy farming, and sometimes cattle are grazing on the fields as well.

In 2011, subsurface drains were installed at the research location at a depth of 70 cm below surface and a drain spacing of 6 m, to facilitate extra infiltration (and drainage) of water in the area. The passive subsurface drainage and infiltration system (PWIS) was only installed in half of the parcel, the other half was used as a reference location. In 2020, at both reference (RF) and PWIS (MS) locations, part of the field was fenced off to exclude cattle. All permanent measurements, as well as grass harvest information, were carried out in these areas (see sections 4.2-4.4). Mowing and fertilization regimes were kept similar to the farmer's practice, except that artificial fertiliser was applied to the parcel, rather than manure.

4.2 Soil properties

Water retention characteristics, used to relate water potential to water filled pore space (WFPS) and hydraulic conductivity, were determined in 2020 in both the reference and PWIS parcel. They were determined in the lab on soil samples from different horizons, using the evaporation method based on Wind (1969). They are given in terms of the Mualem-Van Genuchten expressions (Mualem, 1976; Van Genuchten, 1980), and are provided in the Appendix (10.1) for the measurements as well as for the models. The fitted saturated hydraulic conductivity ($K_{sat,fit}$) was determined based on the evaporation method and shows matrix hydraulic conductivity, whereas measured hydraulic conductivity ($K_{sat,meas}$) also includes the effects of small macropores. In the SWAP-ANIMO simulations, the water retention characteristics of both parcels were assumed identical, and input was slightly adjusted from measured values during model calibration. For PEATLAND-VU, small differences between the fields were made, according to the measurements. The Van Genuchten parameters for this model were changed compared to the measured values to make the modelled soil a bit dryer, since the effect evaporation was not modelled and would lead to an overestimation of WFPS.

Measurements of OM content (determined as loss on ignition, LOI) and dry bulk density were taken at several moments from 2020 onwards, at several depths. A profile of OM density, obtained by multiplication of dry bulk density and OM content, is given in Figure 4, as function of depth. Organic matter density is slightly higher in the reference parcel as compared to the PWIS parcel in the upper soil layers. This may partially explain differences in CO_2 emission from both sites. These differences

in OM density were accounted for in initialization of the SWAP-ANIMO and PEATLAND-VU simulations, but not in the other models.

No new measurements of mineral content were available. Measurements in Hendriks et al. (2013) on the same location show clay contents of 55.5, 19.2, 14.1 and 11.4 % of the dry bulk density for the layers 0-35, 35-45, 45-70 and 70-420 cm below soil surface. These values are used in SWAP-ANIMO for vertical heat transport calculations.

Measurements of pH_{KCl} were obtained at multiple depths and moments in time. There are no significant differences between the two parcels (Figure 4). For PEATLAND-VU the measured pH_{kcl} was used as input, including the minor differences within the measured data. For SWAP-ANIMO, pH_{KCl} was converted to pH_{H2O} using the empirical relation given in Groenendijk et al. (2005) for peat soils, and no distinction was made for the two parcels.

Soil respiration measurements were performed on loosened soil samples taken from multiple depths. An incubation temperature of 20 °C and optimal moisture conditions were used (see Weidner et al. (2023); *this volume*, for more details). The organic matter dissimilation rate, as required for the models, for these samples was estimated assuming an assimilation efficiency of 25% (i.e. 75% of the carbon used by microbes is transformed directly into CO_2, and 25% is incorporated into new organic matter).

As the reference temperature in both PEATLAND-VU and SWAP-ANIMO is 10°C, a temperature correction was applied from 20°C to 10°C, using a Q_{10} factor. The Q_{10} factor is a multiplication factor with which respiration rates increase given an increase in temperature of 10°C (Hendriks, 1991). No new measurements of the temperature response factor were available, so Q_{10} values given in Hendriks et al. (2013) as determined for soil samples for the same site in Vlist were used for this purpose. They report Q_{10} values of 2.7, 3.3 and 2.5, for the layers 35-45, 45-70 and 70-420 cm, respectively.

The temperature-corrected estimates of the organic matter dissimilation rates are given in Figure 4. Also indicated in that figure are estimates of the dissimilation rate reported in Hendriks et al. (2013) for the same location, obtained from undisturbed soil samples measured under optimal soil moisture conditions, as opposed to measurements in disturbed samples under optimal soil moisture conditions as obtained within the NOBV (Report 6). Estimated dissimilation rates were not directly used as input in SWAP-ANIMO, as these rates represent an integral of dissimilation of all available OM pools. Rather, dissimilation rates of the individual OM pools were loosely calibrated, such that the mean yearly dissimilation rate as function of depth in SWAP-ANIMO was in the same range as the measurements (Appendix 10.2). For PEATLAND-VU the dissimilation rate from deeper layers was used as initial value for the model calibration.

The values for Q_{10} reported above were also used in SWAP-ANIMO simulations as input for the temperature response function. In PEATLAND-VU only one Q_{10} value for all the layers is assumed: 2.8 between 10-20 °C. These values are in line with the relation between measured night-time respiration and soil temperatures at 5 cm depth found from chamber measurements (Aben et al. 2023; *this volume*).

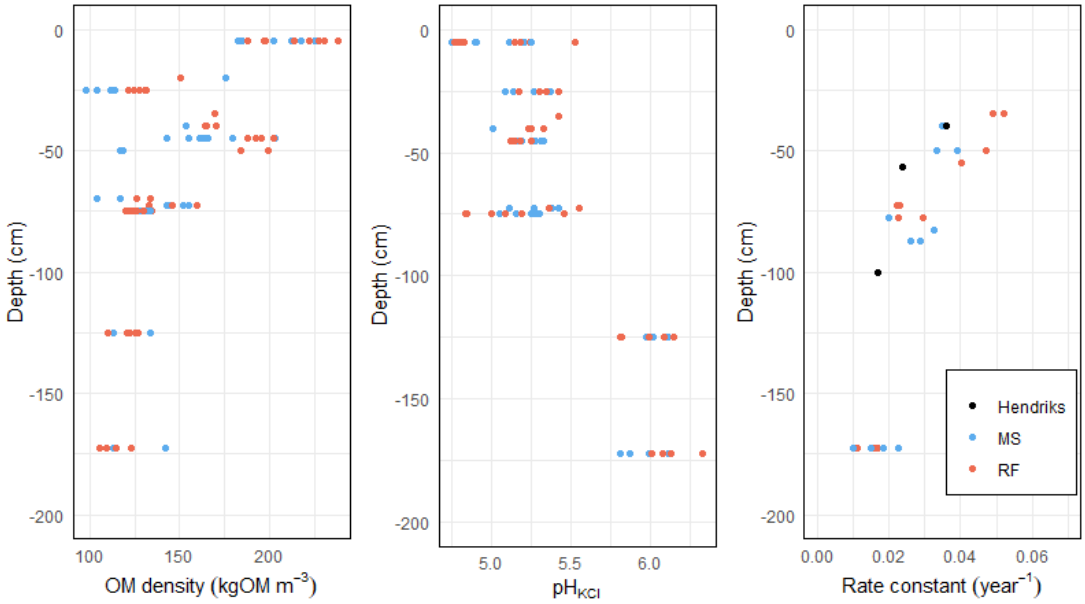

Figure 4 Depth profiles of organic matter (OM) density (left), pH (middle) and potential decomposition rate constant at 10 °C (right) in the reference (RF) and PWIS (MS) parcel. Black dots in the right plot were taken from Hendriks et al. (2013).

4.3 CO_2 flux measurements and flux processing

Fluxes of CO_2 were determined using a set of four automated transparent flux chambers per parcel with a diameter and height of 40 and 50 cm, respectively, which were in place from May 2020 onwards. Chambers were rotated approximately once every two weeks between three locations on the parcel, to reduce effects of chambers on grass growth and local environmental factors. Each chamber was closed once every 15 minutes, for a duration of three minutes, during which the change in CO_2 concentration over time was used to calculate the net ecosystem exchange (NEE). Fluxes were partitioned between gross primary production (GPP) and ecosystem respiration (R_{eco}), following the procedure below, and averaged per parcel over all chambers. In this report, we define both GPP and R_{eco} to be positive, and a negative NEE corresponds to uptake of CO_2, following

$$NEE = R_{eco} - GPP. \quad (3)$$

R_{eco} during daytime was determined using the Lloyd-Taylor equation (Lloyd and Taylor, 1994), which reads

$$R_{eco} = R_{ref} e^{E_0\left(\frac{1}{T_{ref}-T_0}-\frac{1}{T-T_0}\right)}, \quad (4)$$

where R_{eco} [kg CO_2 d^{-1}] is the ecosystem respiration, R_{ref} [kg CO_2 d^{-1}] is the reference respiration during night time, E_0 [K] is the long-term ecosystem sensitivity coefficient, T_{ref} [K] is the reference temperature, T [K] is the actual temperature and T_0 [K] is a base temperature, given as 227.13 K. Daily average night-time fluxes and soil temperature at 5 cm depth were used to obtain a value for E_0 for the whole timeseries per parcel. For each calendar day, measured night-time data was averaged to obtain a daily value of R_{ref} and T_{ref}. An estimate of day-time respiration was calculated using Rref, Tref and measured soil temperatures at 5 cm depth during the day for every 30 minutes. Finally, daily GPP was calculated using Eq. (3). Gap filling of flux data was done by interpolating the Lloyd-Taylor parameters for R_{eco}, and light response curve parameters for GPP. More details on flux measurements and processing can be found in Aben et al. (2023) (*this volume*).

4.4 Additional measurements

Continuous measurements

Phreatic groundwater - and surface water levels (Ellitrack, Leiderdorp Instruments) were registered in hourly time intervals at multiple locations throughout the parcel and surrounding ditch. One measurement of groundwater levels at 3-4 m depth, within the peat layer, was available, and no measurements of the underlying aquifer were available for the modelled period. Soil suction and soil temperature were measured at multiple locations and depths using tensiometers (Teros-32, METER). Volumetric water content, used to determine WFPS and soil temperatures (Drill & Drop, Sentek) were registered in 30-minute time intervals at three locations in the parcel, in 10-cm depth intervals between 5 and 115 cm depth. Volumetric water contents were not calibrated site-specifically, such that absolute values of WFPS could only be derived with a high degree of uncertainty from these measurements. Each 30 minutes, average redox conditions were logged, based on in 1-minute time interval measurements (Paleoterra redox probes, Vorenhout et al., 2011). Based on pore water measurements a normalization was applied to a pH_{KCl} of 5.5. Normalized redox measurements were used as an indication for the presence of oxygen at the measurement depth, based on Boonman et al. (in prep).

Meteorological variables were measured on the reference parcel (MaxiMet GMX500, Gill Instruments; SKR 1840D, Skye Instruments; ARG314, Environmental Measurements Limited), providing average air temperature, humidity and pressure on a 30-minute basis, while wind speed was available in a 1-minute resolution. Photosynthetically active radiation (PAR) and incoming short-wave radiation were recorded in a 1-minute resolution as well. Rainfall was measured with a tipping bucket gauge. If meteorological data was missing, data were gap filled with data from a nearby weather station of the KNMI.

Periodical measurements

Grass was harvested 5 to 7 times during the growing season, depending on the year. Yields were determined on four randomly picked 0.5x0.5 m areas per harvest event. Harvested grass was dried and carbon content was determined. Yields on the chamber locations were estimated by combining harvested grass on the chamber parcels with grass height differences between the parcels with and without chambers, to estimate the effect of the chambers on grass growth. A more detailed description is given in Aben et al. (2023) (*this volume*).

Measurements of pore water, drain water and surface water chemistry were taken at several locations and depths monthly or bi-monthly throughout the measurement period. pH, ammonia, nitrate and dissolved organic carbon (DOC) were among the measurements taken, and they were used in calibration of the SWAP-ANIMO model as well.

Soil surface levels were recorded from 2011 onwards, with the exception of 2016 to 2018. In both the reference and PWIS parcel, three parallel transects across the parcel (35 m) were measured once every year, in early spring. It was assumed that swelling of the soil was at a maximum around that time, due to the precipitation excess in winter. The exact location of these transects was marked, such that always the same transects were measured. From 2020 onwards, each transect was measured four times a year to also measure seasonality in soil surface levels. Measurements of the three transects were averaged per measurement campaign to get an estimate of long-term soil subsidence.

Long-term soil subsidence rates were converted to a yearly average CO_2 loss estimate, using (Van den Akker et al., 2008)

$$R_{soil} = S \cdot fr_o \cdot \rho_{peat} \cdot fr_{OM} \cdot fr_C \cdot \frac{44}{12}, \quad (5)$$

where R_{soil} [kg CO_2 m^{-2} yr^{-1}] is the yearly CO_2 emission from the soil, S [m yr^{-1}] long-term soil subsidence, fr_o [-] the fraction of subsidence caused by peat oxidation, ρ_{peat} [kg m^{-3}] the density of a peat layer, fr_{OM} [-] the fraction of OM in the peat layer (as determined by LOI), fr_C [-] the carbon fraction in the organic matter and 44/12 a conversion factor for C to CO_2.

As estimates of fr_o vary widely (0.28-0.7) between sites as a consequence of e.g., time after first drainage, land use or mineral content (Schothorst, 1982; Leifeld et al., 2011), an alternative approach is used where fr_o is set at 1, and the properties of pristine peat layers are considered in Eq. (5), rather than topsoil properties (Van den Akker et al., 2008). This way, it is assumed that over the subsidence period considered, carbon lost from the topsoil is replenished by carbon from the pristine peat layers, such that the topsoil is in steady state and all soil subsidence is caused by conversion of pristine peat to degraded peat only. This approach is valid only when the onset of drainage of the site was not recent, such that consolidation and shrinkage of the topsoil are of minor importance. Even though minerals are present in the pristine peat layer as well (1-fr_{OM}~0.2), it is assumed that these do not influence the topsoil thickness over a time period of a few decades. This is allowed, as e.g. the removal of 1 m peat with a density of 140 kg m^{-3} and a mineral fraction of 0.2 would, upon oxidation of all peat, leaves a mineral layer of only 0.028 m assuming a mineral soil density of 1000 kg m^{-3}.

5 Results

5.1 Groundwater level

Phreatic groundwater levels as measured between May 2020 and April 2022, and modelled by SWAP(-ANIMO) (January 2020 – April 2022), PP2D(-AAP) and HYDRUS(-AAP) (January 2020-December 2021) for both reference and PWIS parcel are shown in Figure 5. An overview of performance statistics is given in Table 1. For brevity, in the following sections when discussing hydrological results obtained with only the hydrological part of the model, we refer to this part of the model only. Groundwater levels in the PWIS parcel are higher in summer, and lower in winter, due to additional infiltration and drainage, respectively, through the drain tubes. This pattern is visible in all model simulations as well as measurements. As the installation of the drains aims to increase summer groundwater levels through subsurface irrigation, both the measurements and models indicate the measure does function as intended. However, the overall effect is limited due to relatively low ditch water levels and the considerable drain spacing of 6 m.

Both SWAP and HYDRUS simulate average groundwater levels in the reference parcel which are generally too deep during the summer period. In the dry summer (2020), little response to rainfall events is modelled, whereas the response in a wet summer (2021) is too strong in HYDRUS, and rather well predicted in SWAP. PP2D responds much more quickly on rainfall events in summer, and simulates the measured groundwater levels quite well. This pattern is confirmed by the summer statistics (Table 1), with a high standard deviation in water levels in HYDRUS and a too low mean summer level in SWAP. The main reason for the differences in response to rainfall is the modelling of the unsaturated zone in SWAP and HYDRUS from which evapotranspiration may occur and in which precipitation water can be retained, in contrast to PP2D where recharge is a direct input to groundwater. It seems that too much water is retained in the soil matrix in dry periods in the unsaturated zone models. A main explanation for this difference is the presence of macropores in the soil during dry (summer) periods, which facilitate fast transport of precipitation water to deeper soil layers. In winter periods SWAP and HYDRUS simulate groundwater levels in the reference parcel rather well. In contrast, PP2D tends to predict water levels which are too low in this period.

Modelled groundwater levels for the PWIS parcel show an overestimation of their functioning in the HYDRUS model. The infiltration resistance of the drains and surrounding soil results in non-optimal functioning of the drains, which was not accounted for in the HYDRUS model. As a result, predicted water levels are too high in the HYDRUS model during summer, and too low during winter, and there is too little variation over time. This likely results in an overestimation of any beneficial effects of PWIS on peat decomposition. Similar as in the reference parcel, predicted summer groundwater levels are too low in SWAP, although the differences between measurements and model results are less pronounced. PP2D predicts too low winter water levels, but is rather accurate in summer.

An important difference between all models is the applied bottom boundary condition. SWAP was given a fixed head in the underlying aquifer as bottom boundary condition, given a lack of measurements of this head during the modelling period. Instead PP2D used the heads calculated by the LHM (Landelijk Hydrologisch Model) as bottom boundary condition, which therefore do fluctuate in time. HYDRUS used a fixed flux of 0 mm/d for the base model simulation. Of these bottom boundaries, the fluctuating boundary condition has the most dampening effect on phreatic groundwater levels, and the fixed flux has no dampening effect.

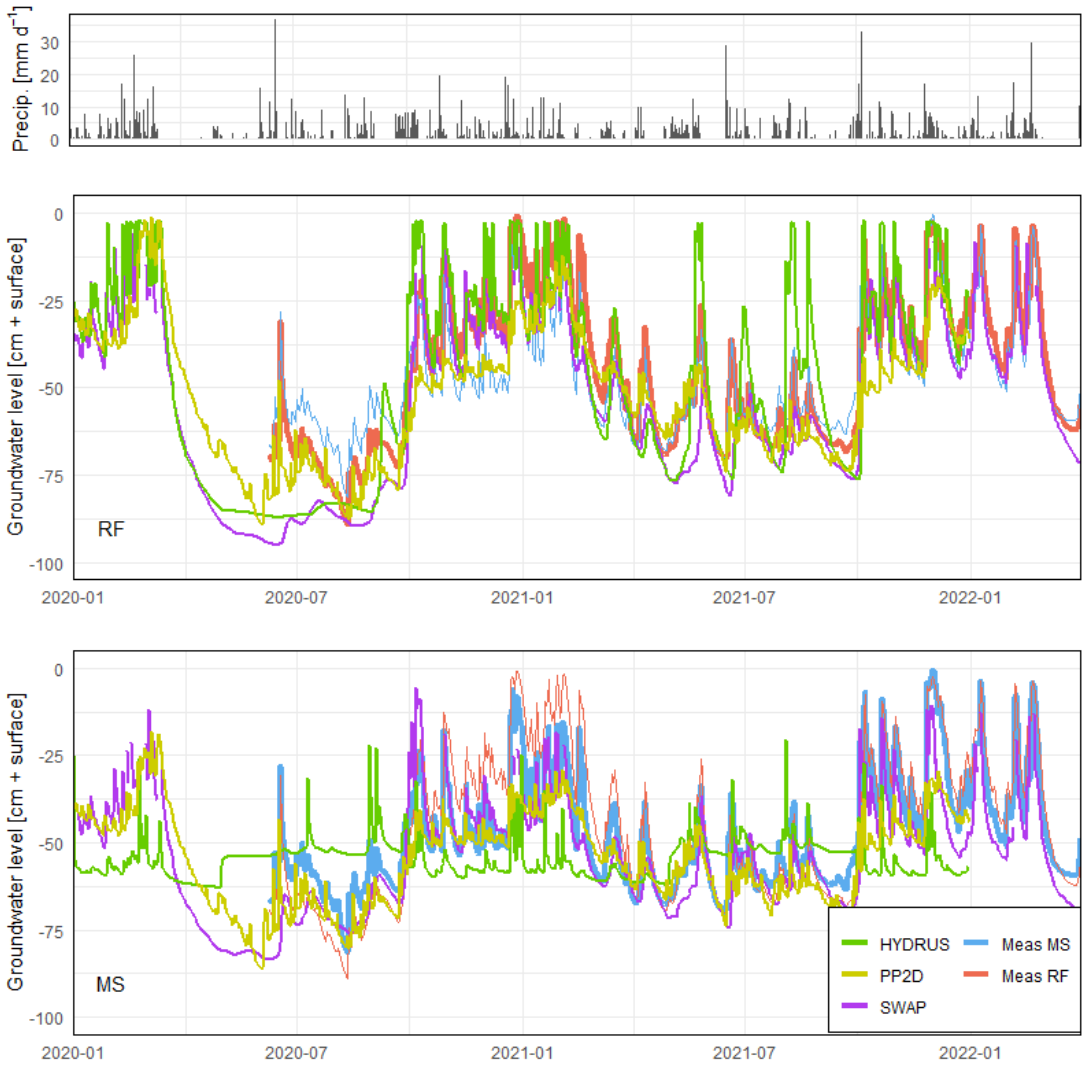

Figure 5 Observed precipitation (upper panel), observed and modelled groundwater levels in the reference parcel (RF, middle panel) and observed and modelled groundwater levels in the PWIS parcel (MS, lower panel). For the purpose of comparison, measured groundwater levels of both parcels are shown in both plots. PEATLAND-VU results are not shown, as measured groundwater levels form input to the model.

Table 1 Water level statistics (in cm) in the reference (RF) and PWIS (MS) parcels for the period May 2020 – December 2021. Shown are the mean water levels in winter periods (October – March) and summer periods (April – September), and the standard deviation over these periods in brackets. Also shown is the RMSE as difference between model results and observations, over the entire period considered.

	Winter period		**Summer period**		**RMSE**	
	RF	**MS**	**RF**	**MS**	**RF**	**MS**
Observations	-35 (19)	-41 (15)	-62 (11)	-59 (8)	-	-
SWAP-ANIMO	-41 (22)	-45 (16)	-74 (12)	-65 (9)	12.9	10.0
HYDRUS-AAP	-35 (21)	-55 (6)	-65 (22)	-52 (6)	14.2	17.1
PP2D-AAP	-46 (15)	-49 (10)	-66 (10)	-64 (7)	12.1	11.3

5.2 Water filled pore space

Water filled pore space (WFPS), the fraction of pores which is filled with water, is important in both PEATLAND-VU and the AAP models in determining the reduction factor due to water (drought) or oxygen limitation of organic matter breakdown. In SWAP, it is important in oxygen transport through the soil as well. Even though measurements of the WFPS were available, they could not be used to determine the absolute WFPS. Therefore, pressure head measurements by tensiometers were translated to WFPS by using the site-specific Mualem-Van Genuchten parameters (Appendix; section 10.1) to be able to compare model results with measurements. Measurements from tensiometers were only available from May 2021 onwards, hence only WFPS simulated and measured in a relatively wet year can be compared at this time. Also note that these Mualem-Van Genuchten parameters were not determined at the exact same location and depth as the tensiometers, and hence also the translation introduces uncertainty in measurements, and that the actual depth of the tensiometer may deviate slightly from the reported depth, due to both the installation procedure and seasonal soil movement.

A comparison between simulated and measured WFPS at 30 cm depth in both the reference and PWIS parcel is shown in Figure 6. Simulated WFPS in PEATLAND-VU is higher compared with tensiometer measurements and other model results. This is partly caused by the assumed hydrostatic equilibrium at all timesteps, i.e. no effects of precipitation and evapotranspiration are considered. Another reason is that some of the van Genuchten parameters in PEATLAND-VU were estimated by the comparing model results with the (not site specifically calibrated) WFPS measurements. These measurements show a higher WFPS compared to tensiometer data (see Appendix; Figure A 1). Also, as organic matter respiration rates are calibrated in PEATLAND-VU, a somewhat higher reference rate may compensate for the relatively high water contents as the water contents do follow a similar pattern as measured water content. Simulation results from SWAP, HYDRUS and PP2D compare quite well to measurements in both the PWIS and reference parcels. For locations deeper in the profile, WFPS essentially follows groundwater level fluctuations. For shallower depths, the influence of evapotranspiration and precipitation on WFPS and soil water pressure become even more evident. Measured and modelled WFPS at 20 cm depth (Appendix; section 10.4) give a similar (but drier) pattern as in Figure 6, but do show that PP2D tends to underestimate WFPS during summer 2021.

All models predict a higher WFPS in the PWIS parcel as compared to the reference parcel during summer at shallow (<30 cm) depths. However, observations suggest that WFPS at these depths is generally lower in the PWIS parcel as compared to the reference parcel. In general, a similar pattern is observed in other paired field sites within NOBV. This may be caused by differences in soil physical conditions between both parcels, influencing the translation from pressure head to WFPS with the Mualem-Van Genuchten expression. However, not only WFPS but also pressure heads are lower in the PWIS parcel compared to the reference parcel during summer. Differences may be attributed to potentially slightly different sensor placement depths. Another explanatory factor may be related to differences in onset of grass growth. As soils are slightly drier in the PWIS parcel as compared to the reference parcel at the onset of spring, grass growth and therefore transpiration may start earlier in the PWIS parcel, resulting in faster drying of the upper soil layers. Upon rainfall, hysteresis in drying and wetting of the soil, and formation of macropores (both processes not accounted for in any of the models) may result in a lasting effect throughout the summer. Neither is the enhancement of infiltration by cracks in the soil that form in dry periods included.

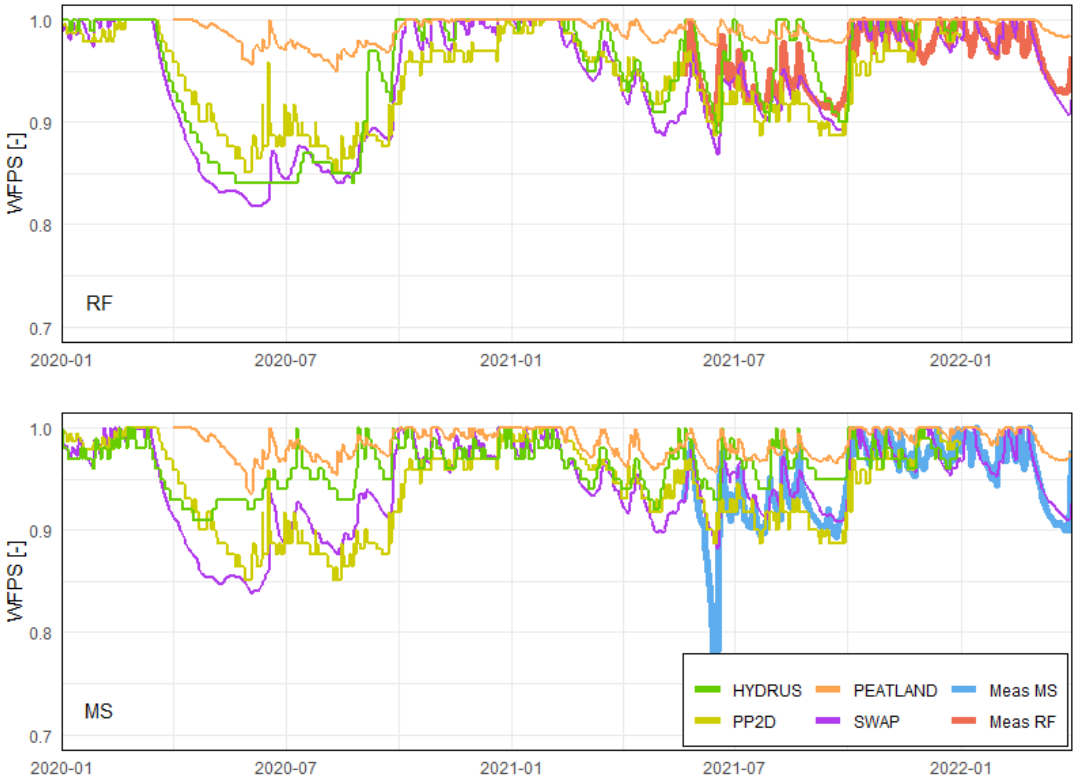

*Figure 6 Modelled and observed water filled pore space (WFPS) at 30 cm depth in the reference (upper) and PWIS (lower) parcels. Observations are translated from pressure heads recorded by tensiometers using the Van Genuchten functions with parameters given in the Appendix (*10.1*).*

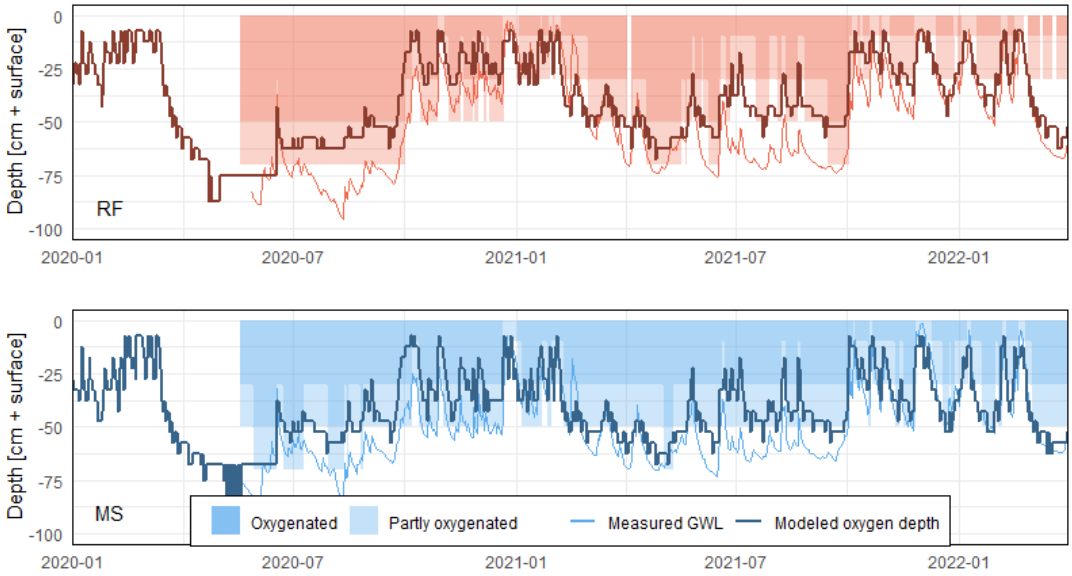

Figure 7 Development of oxygen penetration depth over time, based on redox measurements at a 20 cm depth interval (shaded area) and the SWAP-ANIMO model (thick line), for the reference (RF, upper) and PWIS (MS, lower) parcels. The dark shaded area indicates the region in which oxygen is available according to the measurements, the light shaded area indicates the region between the lowest oxygenated and the highest non-oxygenated redox sensor, as indication where the actual oxygen penetration depth is situated. Model and measurements align when the modelled penetration depth lies in the light shaded area. Also shown are the measured groundwater levels, indicated by thin lines.

5.3 Oxygen penetration

Oxygen penetration depth as inferred from redox measurements and modelled by SWAP-ANIMO is given in Figure 7. As redox sensors are situated at depth intervals of 20 cm, starting at 10 cm below the soil surface, only a range between which the observed oxygen penetration depth is situated can be inferred from the measurements, which is indicated by the light shaded areas in Figure 7. The oxygen penetration depth is well simulated by the SWAP-ANIMO model, even in situations where the groundwater tables are simulated too deep (summer 2020; Figure 5). Therefore, the overestimation of groundwater depth by SWAP-ANIMO has limited influence on organic matter breakdown in the SWAP-ANIMO model.

The penetration depth of oxygen within the soil is relevant for the potential for aerobic decomposition of organic matter. It is clear from both the measurements and model that oxygen does not always penetrate down to the groundwater table, especially in case of deeper groundwater levels. An anoxic zone remains present above the groundwater table, where aerobic breakdown of organic matter does not occur. Of all models in this report, this process is only accounted for in SWAP-ANIMO. However, given the high WFPS in the proximity of the groundwater table, the other models simulate little breakdown of OM in this region as well.

5.4 Soil temperature

Modelled and measured soil temperatures at 15 and 55 cm depth in the reference parcel are shown in Figure 8. In both models and measurements, the amplitude of the seasonal temperature fluctuation diminishes with depth, and the oscillation wave is shifted in time, as is generally observed for depth-time soil temperature profiles. Only minor differences in measured temperatures in the reference and PWIS parcel can be observed (Figure 8). Therefore, only model results of the reference parcel are shown.

Clearly soil temperatures in PP2D provide a great simplification of the actual soil temperatures at all depths, which may influence estimates of peat decomposition in time. Temperatures simulated with SWAP at a shallow depth exhibit a too strong day to day fluctuation, which is caused by neglecting the influence of radiation on soil temperature. Other models perform better in this respect, which is likely due to the fact that for these models measured soil temperatures at 5 cm depth are prescribed, rather than only air temperatures as in SWAP. Soil temperatures at 15 cm depth are slightly underestimated by SWAP in the summer of 2021, whereas summer temperatures are overestimated by the HYDRUS model in summer 2020. The latter is likely a consequence of the prescribed soil temperatures at 5 cm depth, which were in fact recorded at a different site. Therefore, these findings do not reflect the models capability of modelling temperatures.

At 55 cm depth, the HYDRUS model overestimates autumn temperatures, again in response to too high prescribed temperatures at 5 cm in 2020. All other models (except PP2D) show a slight underestimation of summer temperatures, whereas winter temperatures are modelled very good by these models. Generally, deviations between model simulations and measurements are less than 2°C for all models (except PP2D) at this depth.

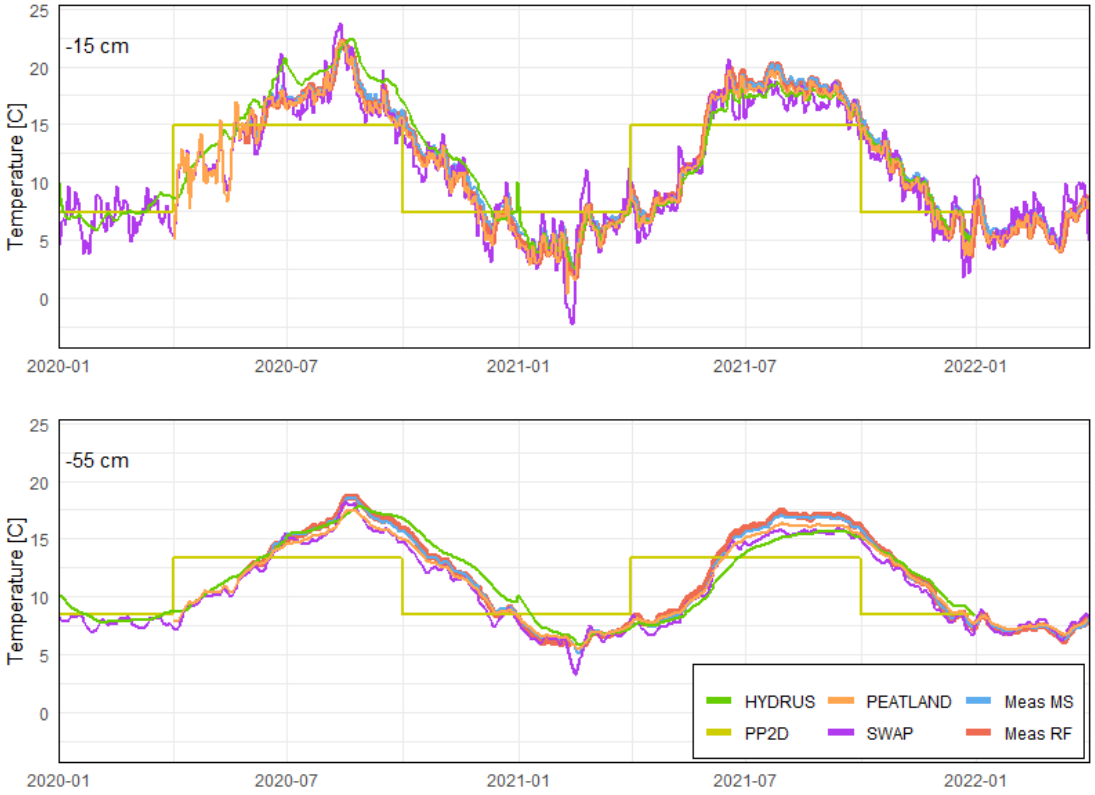

Figure 8 Modelled and measured soil temperatures at 15 (upper) and 55 (lower) cm depth in the reference parcel. Also, measurements of the PWIS (MS) parcel are shown at the respective depths.

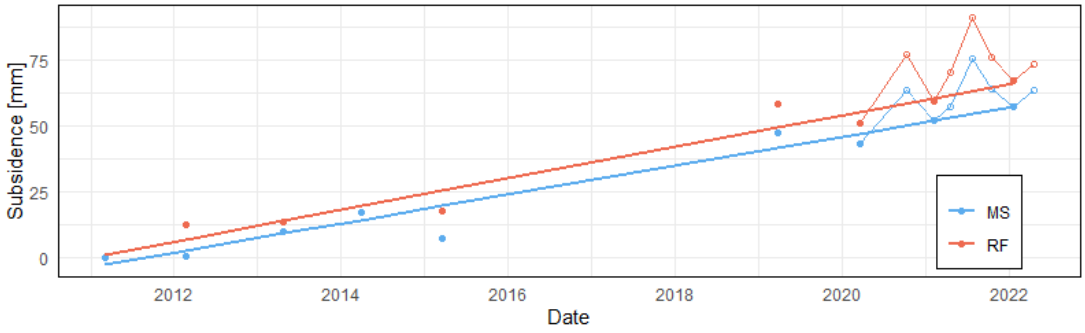

Figure 9 Measured soil subsidence in Vlist on the reference (RF) and PWIS (MS) parcels, based on springtime surface level measurements (filled circles) with fitted linear regression lines (solid thick lines). Within year surface level variability is shown as well (open circles; 2020 onwards).

5.5 Soil subsidence

Measurements of the average soil surface level over a twelve-year period, starting after installation of the drains (2011-2022; Figure 9) in the two parcels indicate a beneficial effect of PWIS on subsidence rates: the subsidence rate is slightly reduced. The observed average yearly subsidence rate is 6.0 (5.4-6.6) mm yr^{-1} in the reference parcel, versus 5.5 (5.0-6.0) mm yr^{-1} in the PWIS parcel, the values in brackets denoting the 95% confidence interval of the linear regression. Given the confidence intervals, we may not conclude that there is any significant difference between the two treatments. Given the surface level fluctuation throughout a year, it is not possible to obtain an exact measure of the surface level subsidence over a specific year.

Within NOBV we have multiple sources of bulk density and carbon content estimates. Using only measurements in Vlist taken at more than 1.2 m below soil surface, the peat density estimates range between 125 and 165 kg m-3, organic matter fractions range between 0.74 and 0.81 and carbon content fractions of organic matter range between 0.47 and 0.53. Assuming all values within these ranges are equally likely, and assuming that the soil subsidence rate estimates given above follow a normal distribution, we may obtain an estimate of the CO_2 emission by applying Eq. (5). For the reference parcel, the estimated CO_2 emission is 12.4 (9.7-15.0) t CO_2 ha^{-1} yr^{-1}, while for the PWIS parcel the estimated yearly CO_2 emission is 11.3 (9.0-13.7) t CO_2 ha^{-1} yr^{-1}. Based on soil subsidence measurements, the estimated reduction in long-term CO_2 emission due to applications of drains thus amounts to 1.1 t CO_2 ha^{-1} yr^{-1}, or 8.9%. Again, we cannot conclude a statistically significant difference between the two treatments.

5.6 Carbon fluxes and yield

The measured net ecosystem exchange (NEE) was partitioned into gross primary production (GPP) and ecosystem respiration (R_{eco}) (see section 4.3 and Figure 1) to distinguish between plant uptake of CO_2 and respiration via plants and soil during daytime. In the models which explicitly model plant growth and photosynthesis (SWAP-ANIMO and PEATLAND-VU), the input of carbon by photosynthesis has a direct effect on respiration from living biomass. It is also the main source of carbon into the different short-cyclic SOM pools, with manure being an alternative source, independent of growth. Note that during the modelling period, no manure was applied. Therefore, it is important to calibrate and validate both GPP and R_{eco} separately, to be able to model the contribution of all SOM pools to the total respiration. Note that GPP and R_{eco} are not simulated by HYDRUS-AAP and PP2D-AAP; hence these two models are not considered in this section.

Seasonal patterns of GPP and R_{eco} are modelled quite well by both PEATLAND-VU and SWAP-ANIMO (Figure 10). Reduction of GPP following a harvest event is clearly visible in both the modelled and measured data. A large discrepancy between modelled and measured values is apparent in April 2020, for which no chamber measurements were available, and these periods were gap filled. Other than that, models and measurements seem to align rather well.

Plotting the cumulative fluxes (Figure 11) allows for a more objective comparison between the models and measurements. In both measurements and model results, GPP and R_{eco} are higher in 2020 as compared to 2021. Also, GPP and R_{eco} are higher in the reference parcel as compared to the PWIS parcel in both model and measurements. PEATLAND-VU almost always underestimates GPP and R_{eco}, except for the PWIS parcel in 2021. SWAP-ANIMO is closer to observed GPP and R_{eco}. Since NEE is the R_{eco} subtracted by GPP (Eq. (3)), the difference in the cumulative NEE between PEATLAND-VU and SWAP-ANIMO is smaller on a yearly basis, but still SWAP-ANIMO is a bit closer to observed cumulative NEE than PEATLAND-VU.

Even though yield estimates were based on a combination of measured yield and measured grass height, they remain quite uncertain. With that in mind, yield is generally well predicted by the models (Figure 12), with on average a slightly overestimated yield by SWAP-ANIMO than for PEATLAND-VU, except for PWIS parcel 2021 (see also section 5.7).

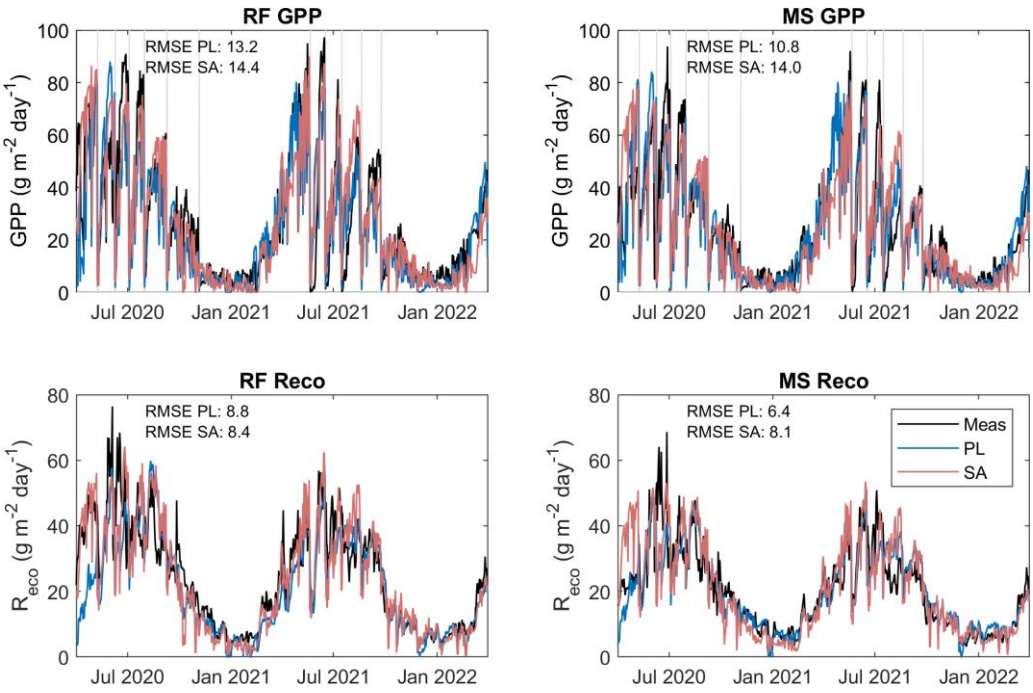

Figure 10 Seasonal patterns of GPP (above) and R_{eco} (below) for the reference (RF) and PWIS (MS) parcel. With grey vertical lines for harvest moments in GPP plots. Measured and modelled data are presented.

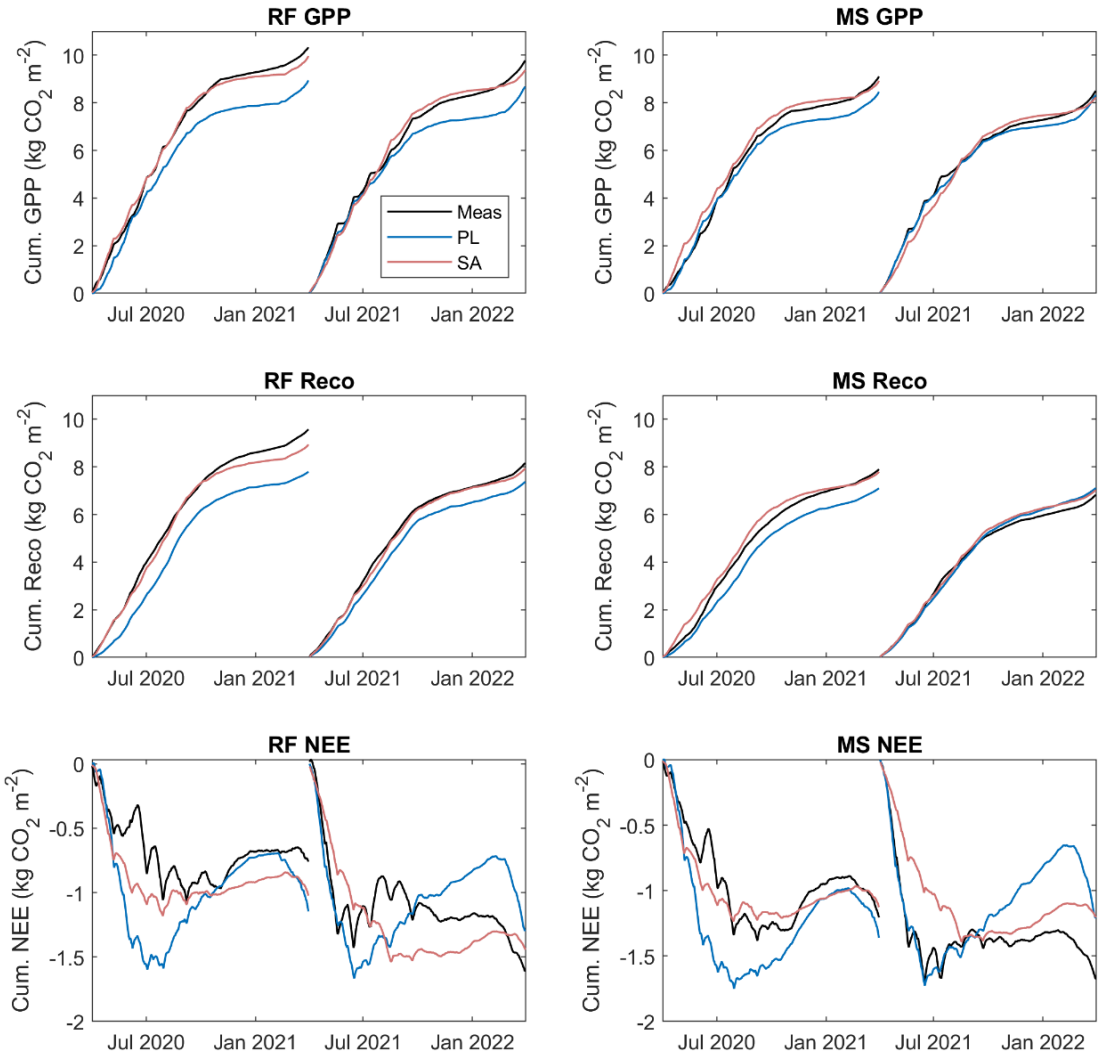

Figure 11 Cumulative GPP, R_{eco} and NEE as measured (black) and modelled in blue (PEATLAND-VU) and red (SWAP-ANIMO) for the reference (RF, left) and PWIS (MS, right) parcels. Two different years are shown, ranging from April 1st to March 31 in the next year.

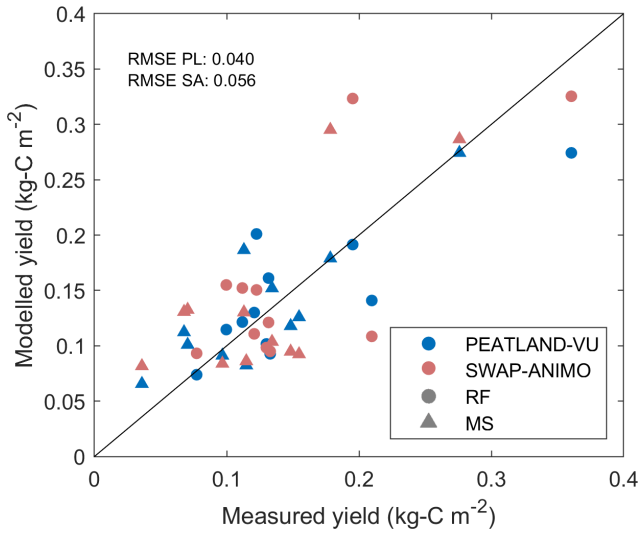

Figure 12 Modelled vs. measured yield for the reference (circles) and PWIS (triangle) parcels. Modelled with PEATLAND-VU (blue) and SWAP-ANIMO (red).

5.7 Carbon year budgets

Summation of NEE and yield (converted to mass of CO_2) provides the net ecosystem carbon balance (NECB). The NECB provides an estimate of the soil organic matter loss (omitting the contribution of exchange in dissolved organic matter and methane), which, on the long term, is thought to be a measure of peat oxidation. We obtained an estimate of the NECB per year for the chamber measurements (Aben et al, 2023; *this volume*) as well as for the models. HYDRUS-AAP and PP2D-AAP only model net loss of carbon (in the form of CO_2) from the soil, presumably omitting any contributions of biomass and biomass-derived SOM. Therefore, their output may be compared to the NECB. We also compare yearly NECB estimates with long-term CO_2 emission estimates based on soil subsidence. To determine the NECB, one would ideally take a year budget over the entire growing season, and have a cut-off point during a period with little plant growth, for instance from January to January. As chamber measurements started only in May 2020, we chose to make year budgets from April to April, using some gap-filled data prior to the onset of chamber measurements. Year budgets of HYDRUS-AAP and PP2D-AAP do range from January to January, as simulations were only available on year-to-year basis, and no data of 2022 was available at the time of reporting.

All models show an NECB in the same range as the measured NECB for both years. The largest discrepancy is observed for the PWIS parcel in 2021, where all models predict a higher NECB than measured (Table 2 and 3). Models predict a slightly higher NECB than measured in 2020 as well, but not as pronounced as the year after. As a consequence, the effect of PWIS on the NECB is more pronounced in the measured data as compared to the model results. In 2020 a reduction of 6.6 t CO_2 ha^{-1} (31% of the reference NECB in 2020) is measured, with all models predicting a lower reduction in both absolute and relative sense. In 2021, measurements suggest a reduction of 3.1 t CO_2 ha^{-1} (25%), while the models predict hardly any reduction, or even an increase (HYDRUS-AAP and PP2D-AAP) in emission from the PWIS parcel as compared to the reference parcel in this wet year. Assuming that groundwater levels are a main driving factor of emission (reduction), one would expect the emission reduction in the wet year 2021 to be small: Figure 5 and Table 1 indicate that the beneficial effect of PWIS on groundwater levels is limited during summer, especially in 2021.

We were not able to provide a definitive explanation for the differences in modelled and measured NECB reductions, but it may very well be related to uncertainty in measured yield. Especially in 2021, measured NEE is very well comparable between the reference and PWIS parcel (Table 3), with a difference of only 0.9 t CO_2 ha^{-1}. The majority of the reported difference in NECB thus originates from differences in yield (2.2 t CO_2 ha^{-1}). As the standard deviation in measured yield (2.6 t CO_2 ha^{-1}) is larger than the reported differences in yield between the two parcels, we may also argue that the measurements do not show any (significant) reduction at all for the wet year of 2021, which would be in line with expectations based on reported groundwater levels.

Compared with the long-term averaged carbon losses based on soil subsidence measurements (12.4 t CO_2 ha^{-1} yr^{-1} for the reference parcel and 11.3 t CO_2 ha^{-1} yr^{-1} for the PWIS parcel), both modelled and measured (by chambers) carbon losses given as NECB are significantly higher. The long-term reduction in emission in the PWIS parcel as compared to the reference parcel (1.1 t CO_2 ha^{-1} yr^{-1}) is in the same range as the reduction in NECB modelled in the wet year 2021. Measured NECB reduction for that wet year, however, is still three times as high as compared to the long-term subsidence derived estimates, which further strengthens the hypothesis in the preceding paragraph that uncertainty in the measurements is a main cause for the (apparent) reduction.

Table 2 Yearly CO_2 flux in t CO_2 ha^{-1} yr^{-1} of all NECB components (GPP, R_{eco}, Yield) of both reference (RF) and PWIS (MS) parcel for the year 2020. NEE follows from Eq. (3). Methods indicated with [1] give yearly values from April 2020-March 2021. Methods indicated with [2] give yearly values from January 2020-December 2020. PP2D-AAP and HYDRUS-AAP only model a net loss of CO_2 from the soil, given here as the NECB. The NECB standard deviations presented between brackets include biweekly chamber NEE standard deviations and standard deviations of each harvest measurement.

Field	Method	GPP	R_{eco}	NEE	Yield	NECB	Reduction NECB	
RF	Chamber meas.[1]	103.3	95.7	-7.6	29.2 (2.5)	21.6 (4.7)		
	SWAP-ANIMO[1]	99.7	87.3	-12.4	34.4	22.0		
	PEATLAND-VU[1]	89.4	78.0	-11.4	31.5	20.0		
	PP2D-AAP[2]					18.7		
	HYDRUS-AAP[2]					22.3		
MS	Chamber meas.[1]	91.0	79.0	-12.0	27.0 (1.0)	15.0 (2.7)	6.6	31%
	SWAP-ANIMO[1]	89.2	77.1	-12.1	30.2	18.1	3.9	21%
	PEATLAND-VU[1]	84.6	71.0	-13.6	28.9	15.2	4.8	24%
	PP2D-AAP[2]					18.1	0.6	3%
	HYDRUS-AAP[2]					16.1	6.2	28%

Table 3 Yearly CO_2 flux in t CO_2 ha^{-1} yr^{-1} of all NECB components (GPP, R_{eco}, Yield) both reference (RF) and PWIS (MS) parcel for the year 2021. NEE follows from Eq. (3). Methods indicated with [1] give yearly values from April 2021-March 2022. Methods indicated with [2] give yearly values from January 2021-December 2021. PP2D-AAP and HYDRUS-AAP only model a net loss of CO_2 from the soil, given here as the NECB. The NECB standard deviations presented between brackets include biweekly chamber NEE standard deviations and standard deviations of each harvest measurement.

Field	Method	GPP	R_{eco}	NEE	Yield	NECB	Reduction NECB	
RF	Chamber meas.[1]	98.0	82.0	-16.0	28.6 (2.7)	12.6 (4.6)		
	SWAP-ANIMO[1]	94.3	79.0	-15.3	29.1	13.8		
	PEATLAND-VU[1]	87.1	74.0	-13.1	27.3	14.1		
	PP2D-AAP[2]					15.0		
	HYDRUS-AAP[2]					11.8		
MS	Chamber meas.[1]	85.4	68.5	-16.9	26.4 (2.5)	9.5 (3.4)	3.1	25%
	SWAP-ANIMO[1]	82.7	70.2	-12.5	25.4	12.9	0.9	7%
	PEATLAND-VU[1]	83.6	71.3	-12.3	25.7	13.4	0.7	5%
	PP2D-AAP[2]					15.5	-0.5	-3%
	HYDRUS-AAP[2]					12.3	-0.5	-4%

5.8 Origin of CO_2 respiratory fluxes

Over a period of multiple years, one would expect that all net carbon losses from the ecosystem originate from peat oxidation (excluding transport of DOM), as short-cycle carbon may be assumed to be in equilibrium. Although frequently assumed in the formulation of year budgets, this need not be the case on a year-to-year basis and is definitely not the case on shorter time periods. The use of models allows to disentangle the materials and depths contributing to respiration on shorter time periods as compared to the yearly carbon balance and may give a more accurate estimate of specific peat decomposition instead of the NECB over the year.

PEATLAND-VU and SWAP-ANIMO contain similar SOM pools, like peat, humus, litter and roots, and both consider plant respiration. But there are differences too; PEATLAND-VU has a pool for microbial biomass and root exudates (Figure 2), and on the other hand, SWAP-ANIMO models transport and respiration of dissolved organic matter (DOM) (Figure 3). An overview of the contribution of different pools over time is shown in Figure 13. The contribution of plant respiration and humus are significantly larger in SWAP-ANIMO (although it should be noted that also microbes are part of the humus pool), whereas the contribution of the litter and roots pool is much larger in PEATLAND-VU. It is clear that in spring, the relative contribution of plant respiration to the total respiration is high in both models and decreases as the growing season continues. A main explanation is found in the fact that biomass is highest then and photosynthesis is a strong function of light intensity, thus a peak in GPP is to be expected in June, whereas the peak in soil temperature, as important driver for soil respiration, occurs later, in the second half of summer (Figure 8).

Both models show the highest contribution of plant respiration to the total R_{eco}, amounting to, on average, 60% for SWAP-ANIMO and 46% for PEATLAND-VU (Tables 4 and 5). The other plant derived component which both models have in common, litter and roots, is higher for PEATLAND-VU, with 31% versus 14% for SWAP-ANIMO. Total peat oxidation that directly leads to CO_2 emission amounts to 12% of the modelled R_{eco} for both SWAP-ANIMO and PEATLAND-VU, but the absolute CO_2 production from peat decomposition is on average 12% higher in SWAP-ANIMO relative to PEATLAND-VU owing to the higher overall ecosystem respiration in SWAP-ANIMO (Tables 2 and 3).

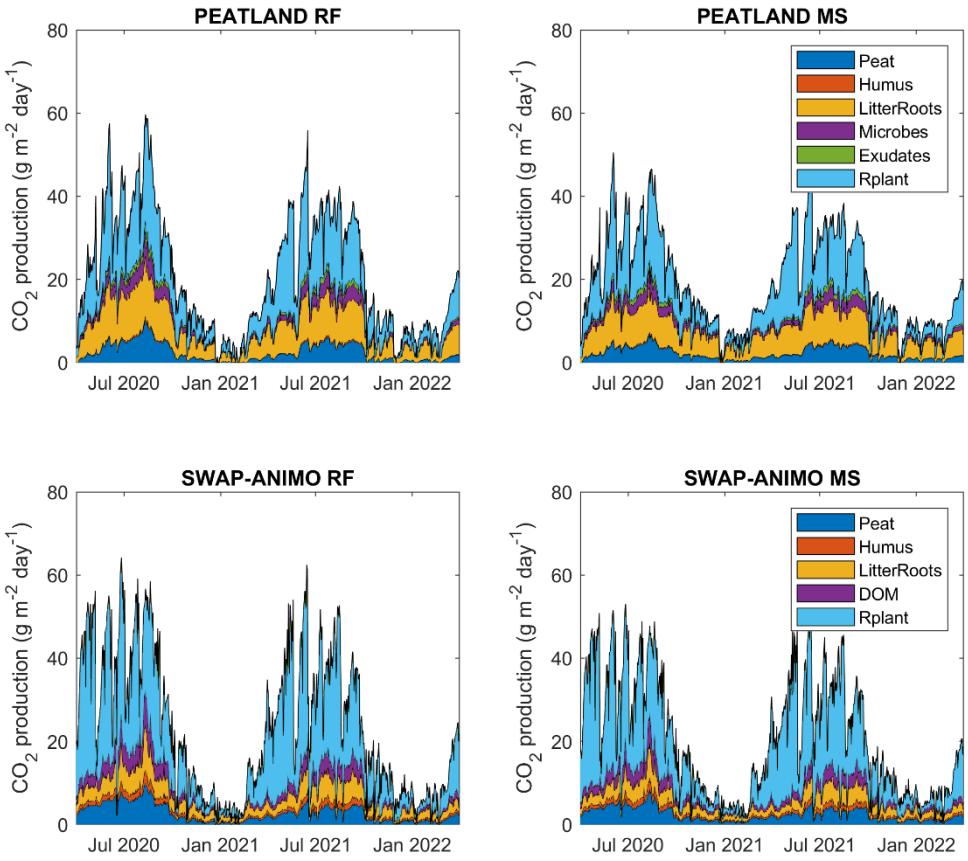

Figure 13 Contribution of different soil organic matter (SOM) pools to the total ecosystem respiration, modelled with PEATLAND-VU (above) and SWAP-ANIMO (below), for the reference parcel (left) and PWIS parcel (right).

CO_2 production from decomposition of peat is not the same as the total CO_2 production related to peat decomposition, since part of the carbon originating from peat decomposition is allocated to other SOM pools (microbial biomass and humus in PEATLAND-VU; DOM and humus in SWAP-ANIMO). This 'fossil' carbon allocated to the other pools will eventually be decomposed to CO_2 as well, but this conversion is subject to different decomposition rates. Microbial biomass has for instance a fast turnover time, while humus decomposition is much slower. In the current model setup of both models, it is not possible to distinguish between the sources of OM after they move from one pool to another, and fossil carbon is mixed with young carbon. To be able to say something about the total fossil carbon emission with the current model setup, we have to assume that the carbon amounts derived from peat decomposition, now present in the other pools, are in equilibrium. This is reasonable as long as either the decomposition rate constant of the pool is higher than the decomposition rate of peat, or if we do not model large fluctuations in the pool over a longer period. The first applies to DOM or microbial biomass, and the second more or less applies to the humus pool. We approximate the total daily CO_2 flux of fossil carbon by multiplying the daily modelled CO_2 loss from the peat pool(s) by a conversion factor, assuming that fossil carbon which is allocated to other SOM pools during a day, is respired from these pools at an equal rate. In PEATLAND-VU, a conversion factor of 1.59, and for SWAP-ANIMO a factor of 1.48 should be used. These values deviate between the models due to different model or parameter assumptions in for instance carbon allocation to different pools, assimilation efficiency or carbon content.

Applying the conversion factors to the modelled carbon fluxes from peat decomposition (Tables 4 and 5), an estimate of peat loss per year is obtained. Averaged over the two years we model an emission due to peat degradation of 14.1 and 12.9 t CO_2 ha^{-1} yr^{-1} for the RF and MS parcel, respectively, with PEATLAND-VU, and 14.9 and 13.4 t CO_2 ha^{-1} yr^{-1} for RF and MS parcel,

respectively, with SWAP-ANIMO. This is well in line with emission estimates based on soil subsidence measurements over a ten-year period, with 12.4 t CO_2 ha^{-1} yr^{-1} for the reference parcel and 11.3 t CO_2 ha^{-1} yr^{-1} for the PWIS parcel (section 5.5). The modelled reduction in emission in the PWIS parcel compared to the reference amounts to 8.5 and 10.0% for PEATLAND-VU and SWAP-ANIMO, respectively, averaged over 2020 and 2021. This is well in line with the reduction estimate based on soil subsidence (8.9%), but is much lower as compared to the measured NECB reduction by chambers (section 5.7).

Comparison of the modelled peat loss with the NECB (Tables 2 and 3) shows that peat losses are lower than the NECB estimates. This may be due to imbalances in the other carbon pools. For SWAP-ANIMO for instance, one of these pools includes the manure pool. As manure was applied prior to the onset of the experiment, but stopped at the moment the parcel was fenced off in 2020, manure residues are still present in the soil and are part of the modelled NECB, but do not contribute to the CO_2 emission due to only peat loss.

Table 4 Modelled CO_2 production per carbon pool for SWAP-ANIMO in t CO_2 ha^{-1} yr^{-1} for reference parcel (RF) and drain parcel (MS) in the two simulated years (2020 = April 2020 – March 2021; 2021 = April 2021 – March 2022). Below the CO_2 production, the contribution of the carbon pool to the total ecosystem respiration (R_{eco}) is given in %.

Field	Year	R_{eco}	Plant	Litter Roots	Peat	Humus	DOM
RF	2020	87.3	49.5 (57%)	12.8 (15%)	12.1 (14%)	3.6 (4%)	9.3 (11%)
RF	2021	79.0	48.4 (61%)	12.0 (15%)	8.1 (10%)	2.1 (3%)	7.5 (9%)
MS	2020	77.1	45.6 (59%)	10.1 (13%)	10.2 (13%)	3.2 (4%)	7.9 (10%)
MS	2021	70.2	43.0 (61%)	9.8 (14%)	7.9 (11%)	2.8 (4%)	6.8 (10%)

Table 5 Modelled CO_2 production per carbon pool for PEATLAND-VU in t CO_2 ha^{-1} yr^{-1} for reference parcel (RF) and drain parcel (MS) in the two simulated years (2020 = April 2020 – March 2021; 2021 = April 2021 – March 2022). Below the CO_2 production, the contribution of the carbon pool to the total ecosystem respiration (R_{eco}) is given in %.

Field	Year	Total R_{eco}	Plant	Litter Roots	Peat	Humus	Root Exudate	Microbes
RF	2020	78.0	34.5 (44%)	24.3 (31%)	9.7 (13%)	0.6 (1%)	2.5 (3%)	6.3 (8%)
RF	2021	74.0	35.3 (48%)	22.4 (30%)	8.0 (11%)	0.6 (1%)	2.1 (3%)	5.6 (7%)
MS	2020	71.0	31.6 (45%)	22.6 (32%)	8.2 (11%)	0.6 (1%)	2.4 (3%)	5.7 (8%)
MS	2021	71.3	32.6 (46%)	22.1 (31%)	8.0 (11%)	0.6 (1%)	2.3 (3%)	5.7 (8%)

5.9 Peat oxidation over time

An overview of the modelled CO_2 emission over time due to peat oxidation is given in Figure 14. It shows rather similar patterns for all four models. PEATLAND-VU and SWAP-ANIMO (showing only the modelled peat oxidation as detailed in the previous section) are very similar, except for the first part of 2020 (where PEATLAND-VU suffers from missing groundwater level data). Also in summer 2021, peat decomposition is slightly higher in PEATLAND-VU as compared to SWAP-ANIMO in both parcels. Peat oxidation for the other two models (HYDRUS-AAP and PP2D-AAP) is given in Figure 14 as well, where the NECB provided in Tables 2 and 3 is divided over the year based on the obtained AAP for these two models. The NECB of gjven by these two models is assumed to consist of only peat oxidation.

Peat decomposition estimates in the reference parcel stand out for the HYDRUS-AAP model in 2020, whereas the decomposition estimates are in line with the other models for the PWIS parcel. This may partly be related to the relatively high temperatures modelled by this model in 2020 (Figure 8), but as a similar pattern emerges in 2021 during a few periods with drier conditions, the model may also be more sensitive to groundwater levels or water filled pore space. The model poorly reproduced the observed groundwater levels, as (Figure 5) too deep groundwater levels were simulated in the reference parcel, and too shallow water levels were simulated in the PWIS parcel. Since the groundwater levels directly affect the WFPS, it is likely that this is the main cause for the relatively high modelled decomposition rates in summer 2020 for the reference parcel. With that, it is also likely that higher simulated groundwater levels in summer would have resulted in a lower reduction in NECB due to drains in especially 2020 (Table 2). Although SWAP-ANIMO also simulates too low groundwater tables in 2020, it is likely that the modelling of oxygen penetration in this model limits the effect of the low groundwater tables (Figure 7).

The effect of the discrete temperature description on the modelled emissions from PP2D-AAP is clearly visible in Figure 14. At April 1st and October 1st, emissions suddenly increase and decrease by approximately a factor 2. It also results in relatively high simulated emissions in between April and June, as actual soil temperatures in that period are considerably lower as compared to the model input (Figure 8). The effect is somewhat concealed in October, as the drop in temperature in both years coincides with a sudden rise in groundwater level around that date.

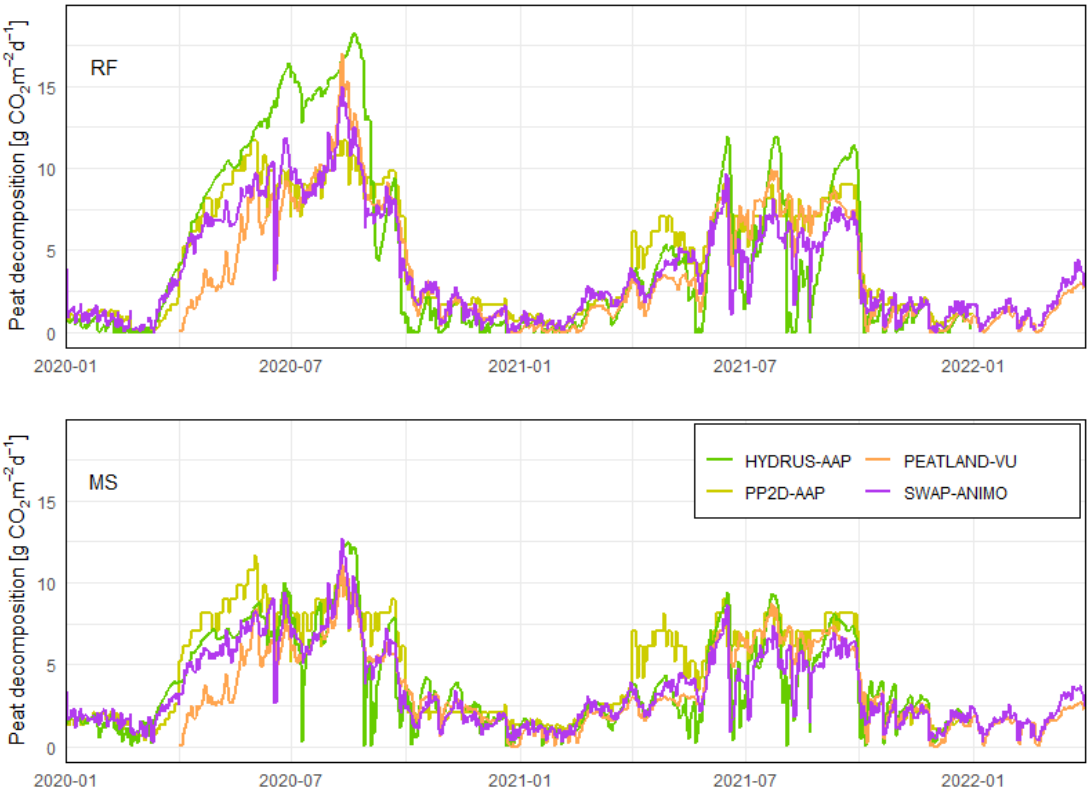

Figure 14 Peat decomposition over time for the reference (upper) and PWIS (lower) parcel. Four model results are shown, where for PEATLAND-VU and SWAP-ANIMO, the total peat derived contribution to CO_2 emission is given, and for HYDRUS-AAP and PP2D-AAP the daily peat decomposition is determined based on the fraction of the daily AAP over the total yearly integrated AAP, multiplied by the yearly NECB.

6 Discussion

6.1 Carbon pools, CO_2 fluxes and peat oxidation

The modelled carbon fluxes (GPP, R_{eco} and yield) are in good agreement with the measured fluxes for both PEATLAND-VU and SWAP-ANIMO. The models are very well capable to simulate the seasonal patterns and magnitude of the fluxes, and can therefore be useful for further analyses like water management or climate scenarios. Both models are calibrated on the measured data, so general applicability of the calibrated parameters needs to be verified on other sites as well.

A large contributor to the carbon budget of the field sites is vegetation. It provides the sole carbon sink (GPP), it is a main way of carbon export from the field through harvest, and ecosystem respiration depends on vegetation through (in order of response time) direct respiration as well as root exudates and decaying plant material. Despite its importance on the carbon budget, quantification of the impact of vegetation on the carbon budget remains challenging, both in measurements and modelling. Nonetheless, it is essential for the interpretation of CO_2 flux measurements on shorter (i.e. less than a year) timescales to disentangle the sources of CO_2 contributing to ecosystem respiration in time.

SWAP-ANIMO and PEATLAND-VU use different approaches to simulate biomass production (see sections 3.1 and 3.2). The models come to an average carbon use efficiency (fraction of GPP that is incorporated into structural biomass) of around 0.58 for PEATLAND-VU and 0.49 for SWAP-ANIMO. This is in line with the 0.4 - 0.6 that Cannel and Thornley (2000) report. Even though there are small differences in the carbon use efficiency, the fraction of GPP that is converted to yield is for both models very similar (Tables 2 and 3). This implies that either less carbon is partitioned to the roots in PEATLAND-VU as compared to SWAP-ANIMO, or that more aboveground biomass dies off in PEATLAND-VU. As the partitioning factor to roots in both models is 30%, the latter is likely the case. This also explains a larger contribution of the litter and roots pool in PEATLAND-VU as compared to SWAP-ANIMO (Figure 13).

The GPP that is not invested in biomass, is used for plant respiration or, in case of PEATLAND-VU, also for root exudates. Plant respiration in PEATLAND-VU is based on a temperature response and leaf area index (surface leaf area per surface of soil), while in SWAP-ANIMO the commonly used (e.g. Cannel & Thornley, 2000) distinction between maintenance and growth respiration is made. Maintenance respiration is a function of actual biomass and temperature, whereas growth respiration is a function of the actual growth, which depends on the availability of assimilates (and thus light). SWAP-ANIMO predicts a higher plant respiration rate than PEATLAND-VU. This is partly because root exudates in SWAP-ANIMO are part of the root respiration rate, but is mainly related to different parameterization of the models. It is, given the available data or literature, at this time impossible to tell whether one or the other model is closer to reality.

The omission of root exudates in SWAP-ANIMO implies that no soil oxygen is used for respiration of root exudates. Comparing modelled root respiration rates to the total modelled respiration from the soil, and assuming that half of the root respiration is actually root exudates (Kuzyakov et al., 2001), up to 20% of the daily soil oxygen consumption modelled in SWAP-ANIMO may actually be required for breakdown of root exudates. This would imply a larger depletion of oxygen in the upper soil layers, and consequently also a lower penetration depth of oxygen into the soil, limiting breakdown of peat in deeper soil layers.

Root exudates and the litter and root pools are the SOM pools that are directly linked to biomass production. Peat is a SOM pool that is independent of the plant production, although in spring a priming effect enhances peat oxidation in the PEATLAND-VU model. When these SOM pools are decomposed, the largest fraction of the decomposed carbon is directly converted to CO_2, and the rest is allocated to the other SOM pools: microbial biomass (27%) and humus (10%) for

PEATLAND-VU, and DOM (10%) and humus (22.5%) for SWAP-ANIMO. Each SOM pool has its own decomposition rate, depending on pH, temperature and WFPS. The distribution factor of the decomposed carbon to other pools, and the decomposition rates of the SOM pools are parameters that were calibrated or obtained from previous studies. These parameters are essential for the outcome of the contribution of the different pools to the total ecosystem respiration. Differences in these contributions can be seen between models (Tables 4 and 5). Despite the differences, peat oxidation for both models amounts to approximately the same relative contribution to the total flux and are in absolute values also very similar, with 14.9 and 14.1 t CO_2 ha^{-1} yr^{-1} for RF, and 12.9 and 13.4 t CO_2 ha^{-1} yr^{-1} for MS.

6.2 Definition of peat for modelling

Any quantification of 'peat oxidation' not only depends on physical and biogeochemical environmental conditions of the peat soils but also on what is understood to be peat. This holds in particular for modelling soils that have undergone ages long drainage, such as the soils modelled here. Peat is organic sediment consisting in which at least a part of the original plant remains that originally formed the peat are still recognisable (Koppisch et al., 2001). Decomposition of peat already starts in the peat forming wetland environment and proceeds rapidly when peat is drained and becomes accessible for oxygen-rich air and other electron acceptors such as nitrate. Long-term drainage results in decomposition of the original peat to humic substances in which no more plant remains are visible. At least in the top layers of the drained peatland soils in the Netherlands – which may have been drained for a millennium (Erkens et al., 2016) it may be impossible to distinguish between completely humified peat, undecomposed peat fragment, humified organic matter from other sources such as organic manure and remains of recent plant fragments. In the Dutch soil classification, the distinction between 'peat', 'peaty' (as an admixture in mineral material) and 'humic' is based solely on quantity of the organic fraction and the amount of fine clay in the soil; if there is less than 15 - 30% organics (depending on clay content) the organic matter is called 'humic', above this level 'peaty', and above 35 – 70% organic matter, it is peat (Locher and De Bakker, 1990).

For the climate effect of CO_2 emissions from soils, it depends whether old, fossil soil carbon (order of decennia or older) is mineralized, or more recently photosynthesized organics. This fossil carbon includes peat, but also may include peat-derived or otherwise old organic matter. Since organic matter age information is not available, for the modelling here assumptions had to be made on the old organic matter content of the topsoil.

For the models, it was assumed that only the loss of OM from the peat pools was responsible for the CO_2 emissions from old fossil carbon. It was assumed that fossil organic material derived from peat degradation, present in the DOM pools and humus pool (Figure 3), was in equilibrium on a yearly basis (i.e. assimilation and dissimilation of peat-derived OM are equal on a yearly basis). As such, CO_2 losses from the turnover of peat-derived OM are accounted for in the OM loss of peat pools.

7 Conclusions

We have shown that both process-based models PEATLAND-VU and SWAP-ANIMO are able to reproduce measured CO_2 fluxes, both on a daily and a yearly scale. Hydrological conditions relevant for breakdown of organic matter can also be modelled accurately by the SWAP-ANIMO model. The models with a less detailed carbon balance description (PP2D-AAP and HYDRUS-AAP) both show somewhat larger deviations with measured CO_2 fluxes, which may partly be related to their implementation of temperature (PP2D-AAP) and drains (HYDRUS-AAP), respectively.

Comparing the NECB of the chamber measurements with modelled values of the NECB shows that models estimate a higher NECB of the PWIS parcel as compared to the measurements. As a consequence, the estimated reduction in NECB on the PWIS parcel compared to the reference parcel is lower for the models than the measurements, especially in the wet year 2021. However, the modelled peat oxidation and reduction in oxidation on the PWIS site is well in line with long-term soil subsidence measurements.

Flux partitioning in different sources by the process-based models, can be done in terms of short-cycle and fossil carbon pool changes and fluxes. This gives a good insight in the contribution of peat decomposition to ecosystem respiration. Nonetheless, quantification of the exact contribution of the other individual pools remains challenging and differs between models due to differences in model definitions. Also, as we did not measure the contribution of different carbon pools on CO_2 fluxes directly, information from many different sources has to be put together (i.e. basal respiration measurements, literature, calibration). Also, the definition of ‘peat’ may influence the results presented. Modelling additional sites may improve our understanding and feeling of some of the model parameters.

8 Acknowledgements

This study was part of the Netherlands Research Programme on Greenhouse Gas Dynamics of Peatlands and Organic Soils (NOBV), which was launched in 2019 by the Dutch ministry of Agriculture, Nature management and Food quality (LNV) as part of the Climate Agreement. Its objective is to research the effectiveness of measures in peatland areas and to be able to better predict emission levels. The effect on subsidence is also researched. The programme is directed by the Foundation for Applied Water Research (STOWA). The research is conducted by Wageningen University (WU), Wageningen Environmental Research (WENR), Vrije Universiteit Amsterdam (VU), Utrecht University (UU), Radboud University, Deltares research institute.
We thank our colleagues within the NOBV project for fruitful discussions on the modelling of CO_2 emissions, as well as for providing the data required for model calibration. A special thanks to Roel Melman, who reviewed this chapter. We also thank Rob Hendriks for reviewing the SWAP-ANIMO simulations. We thank (former) colleagues of WENR for providing the soil subsidence data. This research was (co-)funded by the WUR internal program KB34 Towards a Circular and Climate Neutral Society (2019-2022), project KB34-005-001 (Peat areas in new circular and climate-positive production systems).

9 References

Aben, R.C.H., Boonman, J., van de Craats, D., Peeters, S., van den Berg, M., Boonman, C., Nouta, R., van Giersbergen, Q., Heuts, T., Erkens, G., van der Velde, Y. (2023) *Effectiveness of subsoil irrigation techniques for reducing CO_2 emissions from drained peatlands.* NOBV report; this volume.

Boogaard, H.L., de Wit, A.J.W., te Roller, J.A., van Diepen, C.A. (2014) *User's guide for the WOFOST Control Centre 2.1 and WOFOST 7.1.7 crop growth simulation model.* Wageningen, Alterra, Report Wageningen University & Research Centre. 133 pp.

Boonman, J., Hefting, M.M., van Huissteden, C.J.A., van den Berg, M., van Huissteden, J., Erkens, G., Melman, R., van der Velde, Y. (2022) Cutting peatland CO_2 emissions with water management practices. *Biogeosciences*, 19(24), 5707-5727, https://doi.org/10.5194/bg-19-5707-2022.

Boonman, J., Harpenslager, S-H., van Dijk, G., Smolders, A.J.P., Hefting, M.M., van de Riet, B., van der Velde, Y. (in prep.) Peatland porewater chemistry reveals field redox ranges for specific decomposition processes.

Cannell, M.G.R., Thornley, J.H.M. (2000) Modelling the Components of Plant Respiration: Some Guiding Principles. *Annals of Botany*, 85(1), 45–54, https://doi.org/10.1006/anbo.1999.0996.

Clerc, M. (2011) From Theory to Practice in Particle Swarm Optimization. *Handbook of Swarm Intelligence*, 3-36, 10.1007/978-3-642-17390-5_1

Erkens, G., Van der Meulen, M. J., Middelkoop, H. (2016) Double trouble: subsidence and CO2 respiration due to 1,000 years of Dutch coastal peatlands cultivation. *Hydrogeology Journal*, 24(3), 551-568, https://doi.org/10.1007/s10040-016-1380-4.

Erkens, G., Melman, R., Jansen, S., Boonman, J., Hefting, M.M., Keuskamp, J., Bootsma, H., Nougues, L., van den Berg, M., van der Velde, Y. (2022) *SOMERS: Subsurface Organic Matter Emission Registration System.* 126 pp.

Groenendijk, P., Renaud, L.V., Roelsma, J. (2005) *Prediction of nitrogen and phosphorus leaching to groundwater and surface waters. Process descriptions of the ANIMO 4.0 model.* Wageningen, Alterra, Report 983. 114 pp.

Hendriks, R.F.A. (1991) *Afbraak en mineralisatie van veen; literatuuronderzoek.* Wageningen, DLO-Staring centrum, Report 199. 152 pp.

Hendriks, R.F.A., Walvoort, D.J.J., Jeuken, M.H.J.L. (2008) *Evaluation of the applicability of the SWAP-ANIMO model for simulating nutrient loading of surface water in a peat land area. Calibration, validation, and system and scenario analysis for an experimental site in the Vlietpolder.* Wageningen, Alterra Report 619. 123 pp.

Hendriks, R.F.A., van den Akker, J.J.H. (2012) *Effecten van onderwaterdrains op de waterkwaliteit in veenweiden. Modelberekeningen met SWAP-ANIMO voor veenweide-eenheden naar veranderingen van de fosfor-, stikstof- en sulfaatbelasting van het oppervlaktewater bij toepassing van onderwaterdrains in het westelijke veenweidegebied.* Wageningen, Alterra, Alterra-rapport 2354. 201 pp.

Hendriks, R.F.H., van den Akker, J.J.H., van Houwelingen, K., van Kleef, J., Pleijter, M., van den Toorn, A. (2013) *Pilot onderwaterdrains Utrecht.* Wageningen, Alterra, Report 2479. 148 pp.

Jansson, P.E., Karlberg, L. (2004) *CoupModel – Coupled heat and mass transfer model for soil-plant-atmosphere systems.* Royal Institute of Technology, Dept. of Land and Water Resources Engineering, Stockholm, TRITA-LWR report 3087. 427 pp.

Koppisch, D, Edom, F., Gelbrecht, J., Augustin, J., Stegmann, H., Koska, I, Zeitz, J. (2001) Prozesse auf Moorstandorten (topische Betrachtung). In: *Landschaftsökologische Moorkunde.* (eds: Succow, M., Joosten, H.), pp. 1-57. Schweizerbart, Stuttgart.

Kuzyakov, Y., Ehrensberger, H., Stahr, K. (2001) Carbon partitioning and below-ground translocation by Lolium perenne. *Soil Biology and Biochemistry* 33, 61-74, https://doi.org/10.1016/S0038-0717(00)00115-2.

Kroes, J.G., van Dam, J.C., Bartholomeus, R.P., Groenendijk, P., Heinen, Hendriks, R.F.H., Mulder, H.M., Supit, I., van Walsum, P.E.V. (2017) *SWAP Version 4; Theory description and user manual.* Wageningen, Wageningen Environmental Research, Report 2780. 244 pp.

Kroes, J.G., Supit, I. (2011) Impact analysis of drought, water excess and salinity on grass production in The Netherlands using historical and future climate data. *Agriculture, Ecosystems & Environment* 144(1), 370-381, https://doi.org/10.1016/j.agee.2011.09.008.

Langevin, C.D., Hughes, J.D., Banta, E.R., Niswonger, R.G., Panday, S., Provost, A.M. (2017) *Documentation for the MODFLOW 6 groundwater flow model* (No. 6-A55). US Geological Survey

Leifeld, J., Müller, M., Fuhrer, J. (2011) Peatland subsidence and carbon loss from drained temperate fens. *Soil Use and Management* 27, 170-176, https://doi.org/10.1111/j.1475-2743.2011.00327.x.

Lloyd, J., Taylor, J.A. (1994) On the Temperature Dependence of Soil Respiration. *Functional Ecology*, 8, 315-323, https://dx.doi.org/10.2307/2389824.

Locher, W.P., de Bakker, H. (1990) Bodemkunde van Nederland, Deel 1. Algemene Bodemkunde. Malmberg, Den Bosch, 439 pp.

Mualem, Y. (1976) A new model for predicting the hydraulic conductivity of unsaturated porous media. *Water Resources Research*, 12(3), 513-522, https://doi.org/10.1029/WR012i003p00513.

Metzger, C., Jansson, P.E., Lohila, A., Aurela, M., Eickenscheidt, T., Belelli-Marchesini, L., Dinsmore, K.J., Drewer, J., Van Huissteden, J., Drösler, M. (2015) CO_2 fluxes and ecosystem dynamics at five European treeless peatlands–merging data and process oriented modeling. *Biogeosciences*, *12*(1), pp.125-146, https://doi.org/10.5194/bg-12-125-2015.

Petrescu, A.M.R., Van Beek, L.P.H., Van Huissteden, J., Prigent, C., Sachs, T., Corradi, C.A.R., Parmentier, F.J.W., Dolman, A.J. (2010) Modeling regional to global CH4 emissions of boreal and arctic wetlands. *Global Biogeochemical Cycles*, *24*(4), https://doi.org/10.1029/2009GB003610.

Shaver, G.R., Street, L.E., Rastetter, E.B., van Wijk, M.T., Williams, T. (2007) Functional convergence in regulation of net CO_2 flux in heterogeneous tundra landscapes in Alaska and Sweden. *Journal of Ecology*, 95, 802-817, https://doi.org/10.1111/j.1365-2745.2007.01259.x

Schothorst, C.J. (1982) *Drainage and behaviour of peat soils.* Wageningen, ICW, Report 3, 18 pp.

Šimunek, J.M., Van Genuchten, M.T., Šejna, M. (2022) *The HYDRUS Software Package for Simulating One-, Two-, and Three-Dimensional Movement of Water, Heat, and Multiple Solutes in Variably-Saturated Porous Media,* PC Progress Hydrus 2D/3D Technical Manual II, 283 pp.

Smith, J., Gottschalk, P., Bellarby, J., Chapman, S., Lilly, A., Towers, W., Bell, J., Coleman, K., Nayak, D., Richards, M., Hillier, J., *et al.* (2010) Estimating changes in Scottish soil carbon stocks using ECOSSE. I. Model description and uncertainties. *Climate Research*, *45*, 179-192, https://doi.org/10.3354/cr00899.

Stolk, P.C., Hendriks, R.F.A., Jacobs, C.M.J., Duyzer, J., Moors, E.J., van Groenigen, J.W., Kroon, P.S., Schrier-Uijl, A.P., Veenendaal, E.M. & Kabat, P. (2011) Simulation of Daily Nitrous Oxide Emissions from

Managed Peat Soils. *Vadose Zone Journal*, 10, 156-168, https://doi-org.ezproxy.library.wur.nl/10.2136/vzj2010.0029.

Van den Akker, J.J.H., Kuikman, P.J., de Vries, F., Hoving, I., Pleijter, M., Hendriks, R.F.A., Wolleswinkel, R.J., Simões, R.T.L., Kwakernaak, C. (2008) Emission of CO_2 from agricultural peat soils in The Netherlands and ways to limit this emission. In: *Proceedings of the 13th International Peat Congress After Wise Use – The Future of Peatlands Volume 1* (eds: Farrell, C., Feehan, J.), pp. 645– 648. International Peat Society, Jyväskylä.

Van Genuchten, M.T. (1980) A closed form equation for predicting the hydraulic conductivity of unsaturated soils. *Soil Science Society of America Journal*, 44, 892-898, https://doi.org/10.2136/sssaj1980.03615995004400050002x.

Van Huissteden, J. (2020). *Thawing permafrost: permafrost carbon in a warming Arctic*. Springer Nature, 508 pp.

Van Huissteden, J., Petrescu, A.M.R., Hendriks, D.M.D., Rebel, K.T. (2009) Sensitivity analysis of a wetland methane emission model based on temperate and arctic wetland sites. *Biogeosciences*, 6, 3035-3051, https://doi.org/10.5194/bg-6-3035-2009

Van Huissteden, J., van den Bos, R., Marticorena Alvarez, I. (2006) Modelling the effect of water-table management on CO_2 and CH_4 fluxes from peat soils. *Netherlands Journal of Geosciences,* 85(1), 3-18, https://doi.org/10.1017/S0016774600021399.

Vorenhout, M., van der Geest, H. G., Hunting, E. R. (2011) An improved datalogger and novel probes for continuous redox measurements in wetlands. *International Journal of Environmental Analytical Chemistry*, 91, 801–810, https://doi.org/10.1080/03067319.2010.535123.

Weidner, S., Keuskamp, J.A., Harpenslager, S-F., Hefting, M. (2023) *Vulnerability of oxidation - Basal respiration and OM stability partitioning*. NOBV report; this volume.

Whipps, J.M. (1990) Carbon economy. In: Lynch, J.M. (ed.): *The Rhizosphere*. Wiley , New York, 59-98.

Wind, G.P. (1968) Capillary conductivity data estimated by a simple method. In: *Water in the unsaturated zone* (Eds: Rijtema, P.E., Wassink, H.), pp. 181-191. Proceedings of the Wageningen symposium, June 1966 ,1. IASH Gentbrugge/ Unesco Paris.

10 Appendix

10.1 Soil physical parameters

The Van Genuchten soil physical parameters determined from measurements on undisturbed soil samples is given in Table A 1, together with the parameters used in SWAP-ANIMO and PEATLAND-VU simulations. Parameters for PEATLAND-VU are estimated based on the comparison between model results and corrected (but not site-specifically calibrated) measured WFPS (Figure A 1).

Table A 1 Water retention characteristics and hydraulic conductivity as measured on three depths per parcel and used as input in SWAP-ANIMO and PEATLAND-VU.

Parcel/model	Depth	θ_{sat}	θ_{res}	α	n	λ	$K_{sat,fit}$	$K_{sat,meas}$
	cm	$cm^3\,cm^{-3}$	$cm^3\,cm^{-3}$	cm^{-1}	-	-	$cm\,d^{-1}$	$cm\,d^{-1}$
RF	15-25	0.70	0.00	0.014	1.17	12.5	5.6	15.5
	45-55	0.87	0.00	0.010	1.21	5.4	22.2	86.9
	65-75	0.92	0.00	0.013	1.26	-1.7	9.8	14.0
MS	15-25	0.72	0.05	0.008	1.24	0.0	0.2	-
	45-55	0.89	0.00	0.011	1.24	1.3	6.1	32.2
	65-75	0.91	0.00	0.017	1.25	1.9	28.0	60.0
SWAP-ANIMO	0-40	0.71	0.00	0.015	1.24	0.0	1.5	15.5
	40-70	0.88	0.00	0.011	1.24	1.3	6.1	30.0
	70-420	0.91	0.00	0.013	1.26	-1.7	9.8	37.0
PEATLAND-VU RF	0-10	0.68	0.38	0.04	1.39	0.0		
	10-30	0.73	0.34	0.007	1.42	0.0		
	30-50	0.84	0.25	0.007	1.96	0.0		
	50-150	0.90	0.27	0.008	1.96	0.0		
PEATLAND-VU MS	0-10	0.69	0.29	0.052	1.39	0.0		
	10-30	0.74	0.23	0.009	1.48	0.0		
	30-50	0.84	0.11	0.009	1.48	0.0		
	50-150	0.90	0.10	0.007	1.96	0.0		

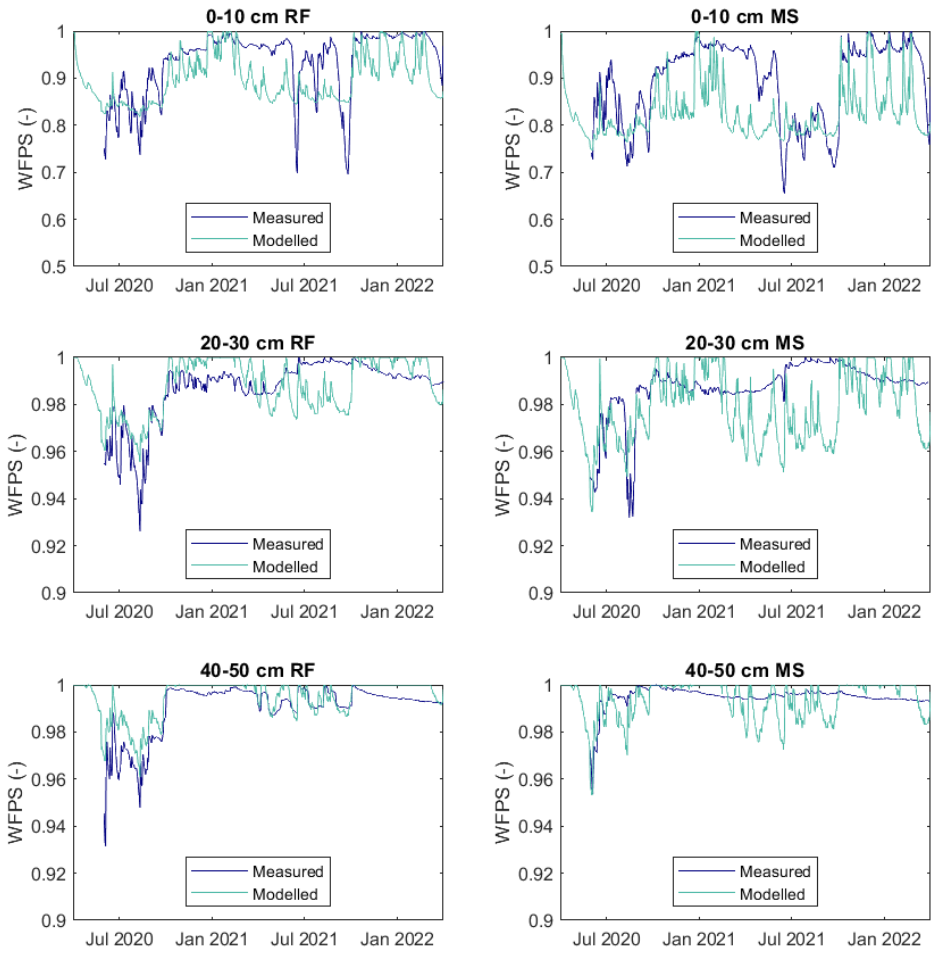

Figure A 1 Measured and modelled water filled pore space (WFPS) with the PEATLAND-VU model for the reference parcel (RF) and PWIS parcel (MS) at three different depths. Measured data are based on direct field measurements, with a correction related to tensiometer data.

10.2 SWAP-ANIMO input parameters

SWAP simulation settings

Half-hourly meteorological input data was used, based on NOBV measurements. A comparison of relevant measurements with the nearby KNMI site Cabauw revealed no biases in the NOBV meteorological measurements. Any gaps in meteorological data were filled with data from the location Cabauw, downscaled from a one hour to half hour resolution.

The soil was discretized in compartments of 1 cm (0-20 cm), 2.5 cm (20-40), 5 cm (40-110), 10 cm (110-200), 15 cm (200-230), 20 cm (230-270) and 25 cm (270-420) thickness. Three horizons were identified (0-40, 40-70 and 70-420) for which the soil physical parameters in Table A 1 were prescribed.

No hysteresis in the soil water retention function was considered. No macropores were simulated. No snow and frost were considered. No solutes were simulated.

Heat transport was modelled with the numerical method, using air temperatures as top boundary and no heat flux as bottom boundary. Given the deviating temperature results (Figure 8), the use of a calibrated relation between top-soil and air temperature is recommended for future work.

SWAP drainage settings

Two (reference) or three (measure) drainage pathways were distinguished (Table A 2). No interflow was considered. Resistances were calibrated based on measured phreatic groundwater levels and soil suction in both parcels, with the constraint that infiltration resistance must be at least as high as drainage resistance.

The bottom boundary water exchange was calculated based on the hydraulic head of the underlying aquifer, with a calibrated resistance. This hydraulic head was fixed in time, as no measurements of this head were available at the time of modelling. Recent measurements (starting in autumn 2022) indicate that the actual hydraulic head in the aquifer shows fluctuations, and may be somewhat higher than used in this study. For future modelling of this site, a relation between the measured hydraulic head at 3-4 m depth and the head in the aquifer may be used to construct an estimate of the aquifer head in the period 2020-2022.

Resistances of the ditch, drain and trench (Table A 2) are much higher (up to a factor 10) compared to general theoretical values for peat meadow areas (Hendriks & van den Akker, 2012). Based on calibration on measured discharge, Hendriks et al. (2013) found relatively large resistances compared to theoretical values for the site in Vlist for the two years after installation of the drains as well. Nonetheless, they are still a factor 2 to 6 smaller as compared to the values in Table A 2. This calls for some additional analysis.

Table A 2 Drainage and infiltration resistances applied in the reference and PWIS parcel. Water levels were prescribed as fixed level (bottom boundary) or variable, based on measurements of ditch water levels. Note: drain parameters only apply to the PWIS parcel.

	Spacing	**Depth**	**Drainage resistance**	**Infiltration resistance**	**Prescribed water level**
	m	m - surf	d	d	m - surf
Bottom boundary	-	4.20	700	700	0.5
Ditch	36.0	1.50	325	350	0.5 to 0.6
Drain	6.0	0.65	300	300	0.5 to 0.6
Trench	18.0	0.15	50	50	-

In situ saturated hydraulic conductivities were measured with the ‘auger hole method’, on 10 locations in both the PWIS and reference parcel. In the PWIS parcel, an arithmetic mean hydraulic conductivity of 0.172 m d^{-1}, and a geometric mean of 0.062 m d^{-1} were found, of which the latter is a better estimate for field averaged hydraulic conductivity.

Based on the drainage theory of Hooghoudt, we can estimate the maximum drain spacing sufficient to discharge enough water given a certain rise in groundwater table. If we take the maximum tolerable head buildup (i.e. increase in head midway between drains with respect to the head inside the drain) of 15 cm for a discharge rate (‘maatgevende afvoer’) of 3 mm d^{-1}, we obtain a resistance of 0.3/15=50 days. Given the measured geometric mean hydraulic conductivity, this corresponds to an optimum drain spacing of 3.3 m, given a thickness of the layer through which flow occurs of 5 m (note: in this specific case, any thickness exceeding 2 m does not change the results). However, the actual drain spacing is 6 m. Therefore, the drainage resistance over this length is much larger than 50 days. The actual resistance is given as

$$r_a = r_e + (r_o - r_e)\left(\frac{L_o}{L_a}\right)^2,$$

where subscripts a, o and e denote actual, optimal and entrance, respectively, and symbols r and L denote the resistance (d) and drain spacing (m), respectively. Assuming the drain entrance resistance to be 10 days, the actual resistance, given the actual drain spacing, equals 141 days. This is much closer to the calibrated value in Table A 2.

The usage of a fixed head as bottom boundary, may have resulted in any additional resistance during the calibration. As the aquifer head also shows seasonal fluctuations, with higher levels during winter, the use of a fixed conditions results in relatively large bottom boundary fluxes, and therefore the model requires drainage fluxes to be limited by a larger resistance. As a monitoring well for the aquifer water level was installed in 2022, it should be possible to improve the calibration in future modelling of this site.

The use of too high resistances for the drains will impact transport pathways of dissolved organic matter in and out of the model in the ANIMO simulations. As groundwater levels were generally well predicted by the SWAP model (section 5.1), the impact on other hydrological conditions is limited.

SWAP crop settings

Grass growth was modelled on both parcels in all years. No grazing was considered and mowing was prescribed to occur on dates with actual harvest events. No delay in start of grass growth was considered, i.e. grass was allowed to start growing on January 1st of each year.

Specific leaf area was specified as function of day number (standard). The standard parameters for light extinction coefficients and light use efficiency were not altered. The maximum CO_2 assimilation rate was prescribed as function of day number using standard parameters for grassland. This rate could be reduced as function of average day temperature and minimum day temperature. The minimum temperature at which CO_2 assimilation could occur was lowered from a standard value of 0°C to -5°C for both reduction functions, as the crop growth model predicted too low GPP as compared to chamber measurements during winter periods.

Conversion efficiency of assimilates into biomass (i.e. the assimilation efficiency) was lowered by 15% compared to standard grassland values, based on comparisons of modelled and measured yield, GPP and ecosystem respiration (Table A 3). Maintenance respiration factors, partitioning factors to roots, stems and leaves and death rates were kept at standard values. Further research in partitioning between growth and maintenance respiration is required, and will be done once additional NOBV sites are modelled.

Rooting depth was kept constant at 30 cm depth, and root density was altered based on root water extraction. This allows roots to move to more profitable locations in the rootzone with respect to water and oxygen availability. Oxygen and water stress were considered based on the Feddes functions. No root water uptake compensation was considered. A CO_2 impact on the growth parameters was considered, as they were initially calibrated for CO_2 concentrations of 360 ppm. The impact of yearly averaged CO_2 concentrations applied to the maximum assimilation rate, light use efficiency and water transpiration. Standard values were used.

Each start of a calendar year, grass was initialized with a total crop dry weight of 1000 kg/ha, partitioned according to the partitioning factors in Table A 3, and a LAI of 0.63 (as is standard for grass). Upon mowing, above ground grass was reset to these values, such that the difference in above ground biomass and the initial conditions was assumed to be harvest. No losses in harvest were considered. A delay in regrowth of the grass after harvest of two to four days was considered, the length depending on the harvested amount.

Table A 3 Partitioning factors (how much of the assimilate goes to which component of the plant), conversion efficiency (how much assimilates are turned into biomass) and maintenance respiration (how much carbon is lost per kg dry weight for maintenance of biomass) for each plant component.

Factor	Unit	Leaves	Stems	Roots
Partitioning	kg/kg	0.42	0.28	0.3
Conversion efficiency	kg/kg	0.6165	0.5958	0.6246
Maintenance respiration	kg CH_2O kg^{-1} d^{-1}	0.030	0.015	0.015

We used parcel and year specific relative management factors to reduce the theoretical potential yield to the maximum attainable yield. For the reference parcel, we used 1.0, 0.97 and 0.90 for the years 2020, 2021 and 2022, respectively. For the PWIS parcel, we used a factor of 0.9, 0.87 and 0.80 for the same years. This factor may deviate depending on the influence of pests (e.g. mice or larvae), nutrient deficit or poor regrowth after mowing (as in 2022). In most cases, it is higher than the recommended factor by Kroes and Supit (2011) of 0.8 for the current nitrogen application rate. This is in line with a lower assimilation efficiency.

ANIMO simulation settings

The ANIMO version used was an adaptation to ANIMO version 4.0 (Groenendijk et al., 2005), considering separate labile and stable dissolved organic matter pools. We simulated diffuse oxygen transport in the soil. We did not make use of the new greenhouse gas module (i.e. no direct simulation of CO_2, CH_4 and N_2O), and did not simulate phosphorus and sulphate or macropores. CO_2 production was, instead, inferred from oxygen (and nitrate-oxygen) consumption output.

The SWAP compartments were upscaled to a size of 5 cm (0-70), 10 cm (70-80), 15 cm (80-110), 20 cm (110-190), 30 cm (190-280), 40 cm (280-320) and 50 cm (320-420) thickness, for which six horizons were distinguished. Input data specified per soil horizon regarding dry bulk density, temperature response factor Q_{10}, pH and oxygen diffusion parameters p1 and p2 are given in Table A 4. Diffusive properties are comparable to values given in Groenendijk et al. (2005) for a soil with good diffusive properties.

Table A 4 Parameters prescribed per soil horizon (H), for both the reference and PWIS parcel. Q10 gives a temperature response factor, and p1 and p2 are parameters which determine diffusive properties of the soil.

Parameter	Unit	H 1	H 2	H 3	H 4	H 5	H 6
Depth	cm-surface	0-5	5-20	20-40	40-70	70-220	220-240
Dry bulk density	kg m^{-3}	480	710	500	225	160	160
Q_{10}	-	2.5	2.5	2.5	3.3	2.7	2.7
pH_{H2O}	-	5.6	5.8	5.8	5.8	6.5	6.5
p1		0.3	0.3	0.3	0.3	0.3	0.3
p2		1.65	1.65	1.65	1.7	1.7	1.7

ANIMO crop and management settings

As the plant module in ANIMO does not use input of the plant module in SWAP, input parameters of the ANIMO model were adjusted to match modelled root zone development in SWAP as closely as possible, while accounting for differences in carbon content between SWAP and ANIMO. In some years, this resulted in an overestimation, and some years an underestimation of decaying root material to the soil. This discrepancy was accounted for in the carbon balance. Harvest was modelled on the same dates as in SWAP.

Manure was applied in the simulation years prior to 2020 (when the parcel was fenced off). Estimates of manure application were based on historical data. From 2020 onward, NPK and N fertilizer was applied, which was used as input for the model.

ANIMO boundary conditions

Top, lateral and bottom boundary conditions were prescribed. The NH_4-N and NO_3-N concentrations in precipitation were set at 0.88 and 0.41 g m^{-3}, respectively, and the dry deposition of these components was estimated to be 8.4 and 1.99 kg ha^{-1} $year^{-1}$. Concentrations of NH_4-N and NO_3-N, dissolved organic matter and dissolved organic nitrogen were set at (a constant value of) 0.05, 0.1, 6.7 and 0.67 g m^{-3}, respectively. The same values were used for the bottom boundary.

ANIMO organic matter settings

We used a carbon content of 0.52 for all organic materials, based on measurements of the subsoil peat in Vlist. Nitrification and denitrification rates were set at 100 and 0.1 y^{-1} and d^{-1}, respectively. An overview of the relevant organic matter pools is given in Table A 5.

Table A 5 Rate constants, fraction partitioned to humus, assimilation efficiency and nitrogen fraction of organic matter for each relevant pool. The fraction (1-assimilation efficiency) is directly converted to CO_2 upon breakdown.

Pool	Sub-class	Rate const.	Fraction to humus	Assimilation efficiency	N fraction
		$year^{-1}$	-	-	-
Fresh Organic Matter	Peat fast	0.0596	0.9[a]	0.25	0.05
	Peat slow	0.003	0.9[a]	0.25	0.021
	Manure fast	1.0	0.75[a]	0.25	0.0706
	Manure med.	0.6	0.75[a]	0.25	0.0706
	Manure slow	0.12	0.75[a]	0.25	0.0706
	Grass shoot	1.5	0.9[a]	0.25	0.04
	Grass root	1.5	0.9[a]	0.25	0.017
Dissolved OM	Labile	100	0.2[b]	0.15	-
	Stable	5	1.0	0.15	-
Humus		0.02	0.96[b]	0.25	0.048

a: Rest moves to labile dissolved organic matter. b: rest moves to stable dissolved organic matter.

ANIMO initialization

Initial conditions of organic matter content of each model compartment are shown in Figure A 2 (compare with Figure 4). Clearly visible is the somewhat higher organic matter content in the reference parcel compared to the PWIS parcel. To initialize organic matter pools in the parcels, we used the SWAP-ANIMO model train to model the periods 1960-1975, 1975-1990, 1990-2000, 2000-2010 and 2010-2020. For the PWIS parcel, drains were only considered from 2010 onwards. Initial conditions in 1960 were such that in the root zone (0-30 cm) 10% of the organic material was humus. The peat (comprising the rest of the organic material) was divided such that 2/3rd of the peat was slowly decomposable, and 1/3rd of the peat was fast decomposable.

During the simulation the total organic matter content decreases due to breakdown of e.g. peat. After each simulation period, therefore organic matter content was restored to the initial conditions, by moving peat upward in the profile. As such, more pristine peat moves upward. This corresponds to the practice of ditch water level lowering after ten to fifteen years, which is required due to land subsidence. For the actual simulation starting in 2020, we initialized the organic matter content once more, such that it agreed with Figure A 2 at the onset of the simulation.

Also shown in Figure A 2 are a comparison between measured and prescribed pH values, and between measured and achieved simulation-averaged (reference) breakdown rate constants as function of depth.

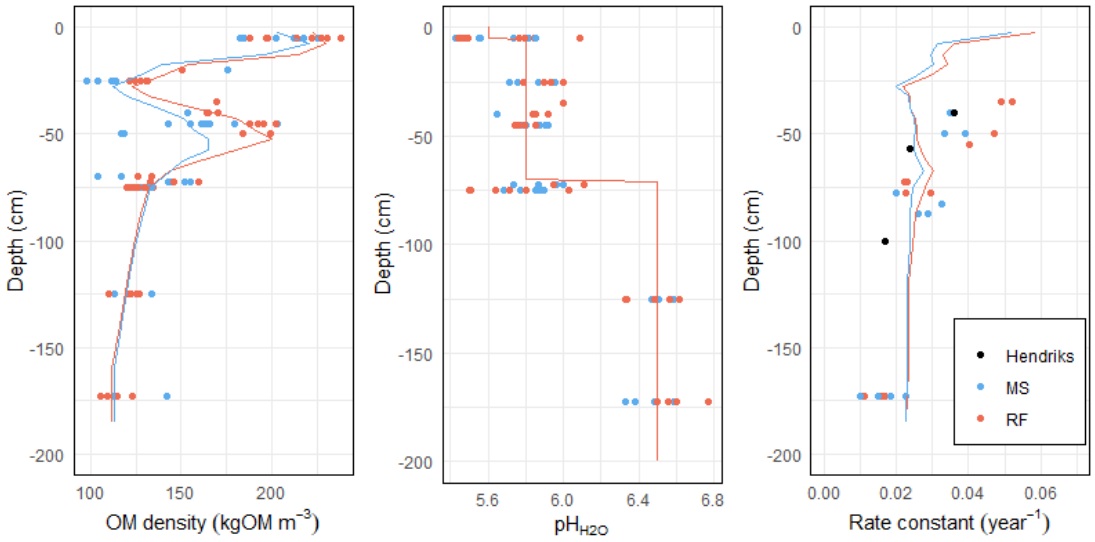

Figure A 2 (left) Organic matter density, (middle) pH$_{H2O}$ and (right) reference breakdown rate, all as function of depth. Dots indicate measurements, lines indicate SWAP-ANIMO input (left, middle) or results (right).

10.3 PEATLAND-VU input parameters

The PEATLAND-VU model was calibrated with the use of measured CO_2 fluxes, partitioned into GPP and R_{eco}, and measured yield. The reference (RF) and PWIS (MS) parcels were calibrated simultaneously, with keeping all parameters the same, except for the biomass production (light response curve and maximal LAI) so that differences in grass growth can be captured. For each parameter the lower and upper limits, and initial value are defined, based on literature or modeller experience. With the calibration, the peat decomposition rate is a bit higher than measured with the basal respiration as described in Weidner et al. (2023) (NOBV report; this volume). This has most likely to do with the lower modelled soil moisture than measured, which is compensated then with a higher decomposition rate.

More information about the calibration method can be found in section 2.1.

Parameter	Description	Initial	Lower	Upper	Result
Kdecay[1]	Peat decomposition rate	0.02	0.004	0.04	0.038
Kdecay[4]	Root exudates decomposition rate	3	1	4	1.44
Kdecay[5]	Litter and root decomposition rate	0.13	0.09	0.3	0.143
Kdecay[6]	Microbial biomass decomposition rate	0.5	0.1	1	0.498
Kdecay[7]	Humus decomposition rate	0.05	0.004	0.07	0.010
ExudateFactor	Exudates release as fraction of NPP	0.34	0.1	0.4	0.239
Klitter	Decomposition rate above ground litter	0.3	0.05	0.5	0.234
PhotoPar[1]	Plant respiration at zero degrees	0.7	0.5	1.5	0.646
PhotoPar[2]	Temp sensitivity plant respiration	0.09	0.06	0.12	0.097
PhotoPar[3]_RF	GPPmax	90	70	100	89.7
PhotoPar[4]_RF	Alpha	0.05	0.02	0.1	0.054
Phenology[2]	base for calculating the heat sum	8	5	10	5.75
Phenology[3]	heat sum when maximum LAI	150	130	170	158
Phenology[4]_RF	maximum LAI	9.5	8	12	11.3
Phenology[6]	fraction biomass littered in autumn	0.8	0.7	0.95	0.926
BioMassSenescence	Fraction above ground biomass	0.025	0.005	0.05	0.013
LAICarbonFraction	Relates leaf area index to biomass	0.06	0.015	0.15	0.101
SatCorr	Correction GPP saturated soil	0	0	0.2	0.035
DryCorr[1]	Correction GPP dryness, VWC wilting point	0.5	0.2	0.7	0.545
DryCorr[2]	Correction GPP, VWC point decrease in GPP	0.8	0.7	0.85	0.724
PhotoPar[3]_MS	GPPmaxlight response curve	90	70	100	91.1
PhotoPar[4]_MS	Alpha light response curve	0.05	0.02	0.1	0.054
Phenology[4]_MS	maximum LAI	9.5	8	12	9.48

10.4 Additional results

WFPS

Figure A 3 shows the estimated (based on tensiometer measurements) and modelled WFPS at 20 cm depth. The measurement at 20 cm depth for the MS parcel was obtained above the drain, and may show somewhat deviating results compared to field averaged conditions. No measurements were available at 20 cm depth further from the drain.

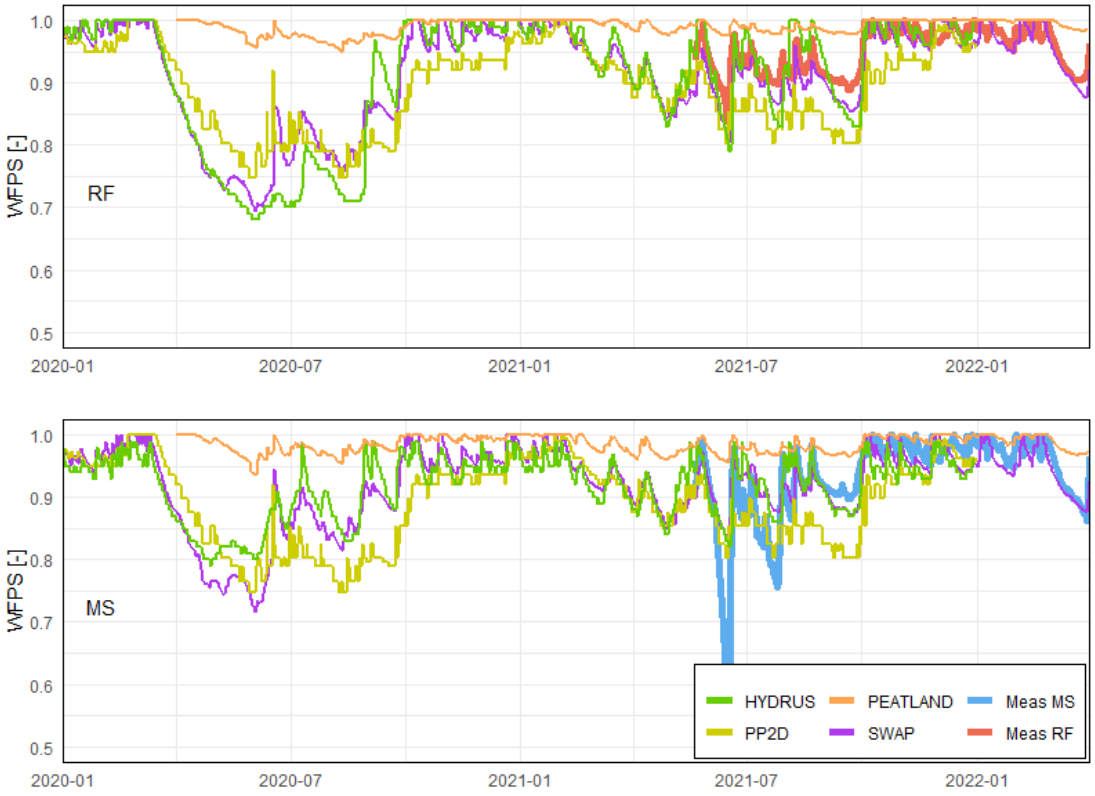

Figure A 3 Modelled and observed water filled pore space (WFPS) at 20 cm depth in the reference (upper) and PWIS (lower) parcels. Observations are translated from pressure heads recorded by tensiometers using the Van Genuchten functions with measured parameters given in Table A 1.

Grass growth

As grass growth is an important contributor to measured and modelled gross primary productivity and ecosystem respiration, we show some modelled and measured grass growth parameters in Table A 6. Unfortunately only yield/GPP could be determined for the chamber measurements, the other parameters are not available as there is no information on below ground biomass.

The ratio of yield over GPP is relatively small in 2020 in the chambers as compared to the models. In fact, models predict a higher ratio in 2020 as compared to 2021, whereas the chamber measurements show a higher ratio in 2021 as compared to 2020. In both models and chamber measurements, the ratio is lower in the PWIS parcel as compared to the reference parcel. Obviously, this impacts the yearly NECB estimates.

The carbon use efficiency (CUE), defined as the total carbon used for biomass growth (and thus not for respiration or root exudates) is higher in PEATLAND-VU as compared to SWAP-ANIMO,

although both fall within literature ranges. The factor death/GPP determines the amount of plant material added to the soil, which is higher in PEATLAND-VU as compared to SWAP-ANIMO. This is in line with higher respiration rates of plant residues in this model. The ratio R_{plant} over GPP is higher in SWAP-ANIMO, which is also in line with the higher plant respiration rates in this model. Finally, a rather large difference in root/shoot biomass is found between the models. This is likely related to more root biomass and less root death in SWAP-ANIMO, and is also related to how harvest is calculated; upon harvest, the ratio root/shoot is impacted as shoots are removed, hence taking more or less shoot material has a significant influence.

Table A 6 Measured (CH) and modelled (SA = SWAP-ANIMO; PL = PEATLAND-VU) crop growth parameters, giving the ratios of modelled plant respiration (including root exudates) over GPP and modelled or measured yield over measured GPP. The remaining fraction (death over GPP) is assumed to be dead biomass (mainly roots, but also some above ground material) which is incorporated into the soil. The carbon use efficiency (CUE) is the fraction of GPP which is actually used in biomass production, and is equal to 1-Rplant/GPP. The modelled yearly averaged root over shoot ratio is given as well.

Parcel	Year	Method	R_{plant}/GPP	Yield/GPP	Death/GPP	CUE	Root/shoot biomass
RF	2020	CH		0.297			
		SA	0.511	0.346	0.143	0.489	1.107
		PL	0.414	0.352	0.234	0.586	0.561
	2021	CH		0.319			
		SA	0.518	0.308	0.174	0.482	0.955
		PL	0.430	0.313	0.257	0.570	0.540
MS	2020	CH		0.277			
		SA	0.523	0.338	0.139	0.477	1.013
		PL	0.402	0.341	0.257	0.598	0.611
	2021	CH		0.297			
		SA	0.520	0.309	0.171	0.480	0.878
		PL	0.418	0.307	0.275	0.582	0.593